AN ANALYSIS OF A MICROSTRIP DEVICE AS A MOISTURE SENSOR FOR GRAIN

by

PAUL WALTON HEIN

Bachelor of Science in Electrical Engineering

Oklahoma State University

Stillwater, Oklahoma

1985

Submitted to the Faculty of the
Graduate College of the
Oklahoma State University
in partial fulfillment of
the requirements for
the Degree of
MASTER OF SCIENCE
July, 1987

AN ANALYSIS OF A MICROSTRIP DEVICE

AS A MOISTURE SENSOR FOR GRAIN

Thesis Approved:

R. Ramakumar.

Thesis Adviser

Bennett Basore

Richard L. Cummins

Norman N. Durham

Dean of the Graduate College

ACKNOWLEDGMENTS

This thesis would not have been possible without the inspiration and help of many individuals. First of all, I wish to give my sincere appreciation to Dr. R. Ramakumar, my thesis adviser, for his expertise and patience in helping me with this thesis. I would also like to thank Dr. Marvin L. Stone, a committee member and a Professor in the Oklahoma State University Agricultural Engineering Department, for the idea and financial support from his department to investigate fringe-field devices as moisture sensors. Dr. Stone's insights and considerations on the difficulties encountered in this research are gratefully appreciated. I also appreciate the help and guidance of the other members of my committee, Dr. Richard L. Cummins and Dr. Bennett L. Basore.

A special person in my life who deserves an enormous amount of recognition is my wife, Becki. Her love and devotion has been a constant means of inspiration to both my personal and scholastic endeavors. I am very grateful for the many selfless sacrifices she has made in typing this thesis.

Finally, I would like to thank my family and friends for their support and confidence in my ability to complete my graduate studies.

TABLE OF CONTENTS

LIST OF TABLES

LIST OF FIGURES

LIST OF SYMBOLS

a,b	- Constants in Equation (1-3-1).
α_{opt}	- Optimum overrelaxation factor, Equation (2-3-26).
C	- Capacitance, F.
c	- Constant in Equation (2-3-27).
c	- Constant in Equation (2-3-28).
$d\overline{L}$	- Differential line element, Equation (2-3-7).
dN	- Normal component of electric flux density, Equation (2-4-2).
$d\overline{S}$	- Differential surface element, Equation (2-3-6).
∇^2	- Laplacian operation.
E	- Inherent error term, Equation (2-3-28).
E_n	- Normal component of electric field, Equation (2-4-1).
$\overline{E}$	- Vector electric field.
ε_o	- Permittivity of free space, $10^{-9}/(36\pi)$, F/M.
f	- Mathematical function.
h	- Elemental length.
h	- Height, Figure 6.
i,j	- Indexis.
J	- Current density, Coul./M^2.
k	- Constant of iteration.
k'	- Relative dielectric constant ($\varepsilon'/\varepsilon_o$).
k''	- Relative loss factor ($\varepsilon''/\varepsilon_o$).

L	- Length.
m	- Slope of regression, pF/MC.
M	- Mass of wheat sample, G.
MC	- Moisture content, percent wet basis.
ρ	- Line charge density, Coul./M .
ρ_b	- Bulk Density, G/CM^3.
Q	- Electric charge, Coul., Chapter II.
Q	- Surface charge density, Equation (2-4-3).
R	- Resistance, ohms.
$R_{i,j}$	- Residual at point (i,j), Equation (2-3-24).
R^2	- Coefficient of determination, Equation (3-3-1).
S	- Surface.
$S.F.$	- Sensitivity Factor, Equation (2-3-4).
SS_R	- Regression sum of squares, Equation (3-3-1).
S_{YY}	- Sum of squares, Equation (3-3-1).
φ	- Scalar potential function, volts.
ϵ_o	- Permeability of free space, $4\pi(10^{-7})$ H/M.
V	- Volts.
$V(m)$	- Variance of slope m.
w	- width, Figure 6.
W	- Mass of water, G, Equation (3-2-2).
x,y	- Cartesian coordinate system variables.
G	- Conductivity, mho.
ω	- Radian frequency.

CHAPTER I

INTRODUCTION

The objective of this research is to investigate the use of a fringe-field device to sense changes in the moisture content in wheat. Commercial capacitance-type moisture meters typically incorporate some form of a 'closed' capacitance cell as the moisture sensing device. As an alternative, this research proposes an 'open' cell configuration, namely, a fringe-field device. Since closed-form solutions for these geometries are usually quite complex, a numerical approximation of this problem is presented. The first chapter reviews the basic electrical properties of grain and the exploitations of these properties to measure moisture content.

1.1 General Literature Review

Moisture content is one of the most critical factors affecting the harvesting, storing, and processing of agricultural products. In addition, moisture content is an important constituent in determining the grade and test weight of grain. Rapid measurements of moisture content are particularly essential during the drying and milling processes. Due to the dependency of the

dielectric properties of grain on the grain moisture content, electric-capacitance type moisture meters use the capacitance cell as the moisture sensor.

1.2 Electrical Properties of Grain

Electrical properties of materials are generally classified into two broad groups: active and passive. The properties in the active group are characterized by their influences as a source of energy in the material. In crystals, for example, the piezoelectric effects of changing mechanical energy into electrical energy and vice versa would be considered an active property. Passive electrical properties are those properties of a material which affect the currents and electric fields in the material. Both the active and passive properties are intrinsic to the material, and they depend heavily upon environmental influences. To study the interactions of electromagnetic energy with matter, a subclass of these properties has been developed. The constituents of this subclass are: permittivity, permeability, and conductivity.

The permeability, μ , of most agricultural products has been found to be very close to that of free space, μ_o. Additionally, moisture content was observed to have little influence on changing the permeability of grain [1].

As derived in circuit theory, permittivity, ε^*, and conductivity, σ , can be expressed in complex form as

$$\varepsilon^* = \varepsilon' - j\varepsilon'' \qquad (1\text{-}2\text{-}1)$$

where the dielectric loss factor, ε'' , is written as

$$\varepsilon'' = \sigma/\omega \qquad (1\text{-}2\text{-}2)$$

The term ε' is known as the dielectric constant. The expression 'constant' is somewhat misleading. Actually, ε' and ε'' depend heavily on moisture content, frequency, and bulk density. Variables of less influence are temperature, nonhomogenity of grains, sorption-desorption cycles, and chemical composition [2]. Throughout the remainder of this study, ε' and ε'' will be expressed in terms relative to the permittivity of free space, $\varepsilon_\circ$;

$$k' = \varepsilon'/\varepsilon_\circ \qquad (1\text{-}2\text{-}3)$$

and

$$k'' = \varepsilon''/\varepsilon_\circ \ . \qquad (1\text{-}2\text{-}4)$$

The complex relative permittivity becomes:

$$k^* = k' - jk'' \ . \qquad (1\text{-}2\text{-}5)$$

1.2.1 Permittivity and Loss Factor

The dielectric constant, k' , of grain has been shown to be positively correlated with moisture content. This dependency can be expected since the dielectric constant of water is very high in relation to the dielectric constant of dry grain [1]. In an experiment using hard red winter wheat, Nelson [2] observed that as the moisture content in the grain increased, the grain's dielectric constant also monotonically increased. In addition, this correlation existed over a wide frequency bandwidth ranging from 250 Hz

to 12 GHz. The k' versus frequency curves for a fixed moisture content behave fairly uniformly in the upper frequency range, 1 MHz up through the microwave band [2]. Figure 1 shows several contour plots of k' and k" of hard red winter wheat as functions of frequency and moisture content. Behaving less predictably, the dielectric loss factor, k" , tends to increase in some instances and decrease in others with respect to frequency and moisture content as variables [2].

Two basic electrical-circuit models are available to represent the effects of k' and k" : the lumped circuit model and the distributed circuit model. When dealing with high frequencies, distributed circuit models are preferred since they represent the high frequency effects more accurately than the lumped models. Distributed models are typically derived from field theory, and an excellent discussion of this is given in a classic text by von Hipple [3].

The lumped RC circuit model can also be used in determining the empirical values for k' and k". The inductance term is omitted in this model since the permeability, μ, of most agricultural products is very close to that of free space. Figure 2 shows the schematic for the parallel RC equivalent circuit.

The capacitive element, C, of the RC circuit represents the charge storing capacity of the dielectric medium confined within the capacitance cell. When the

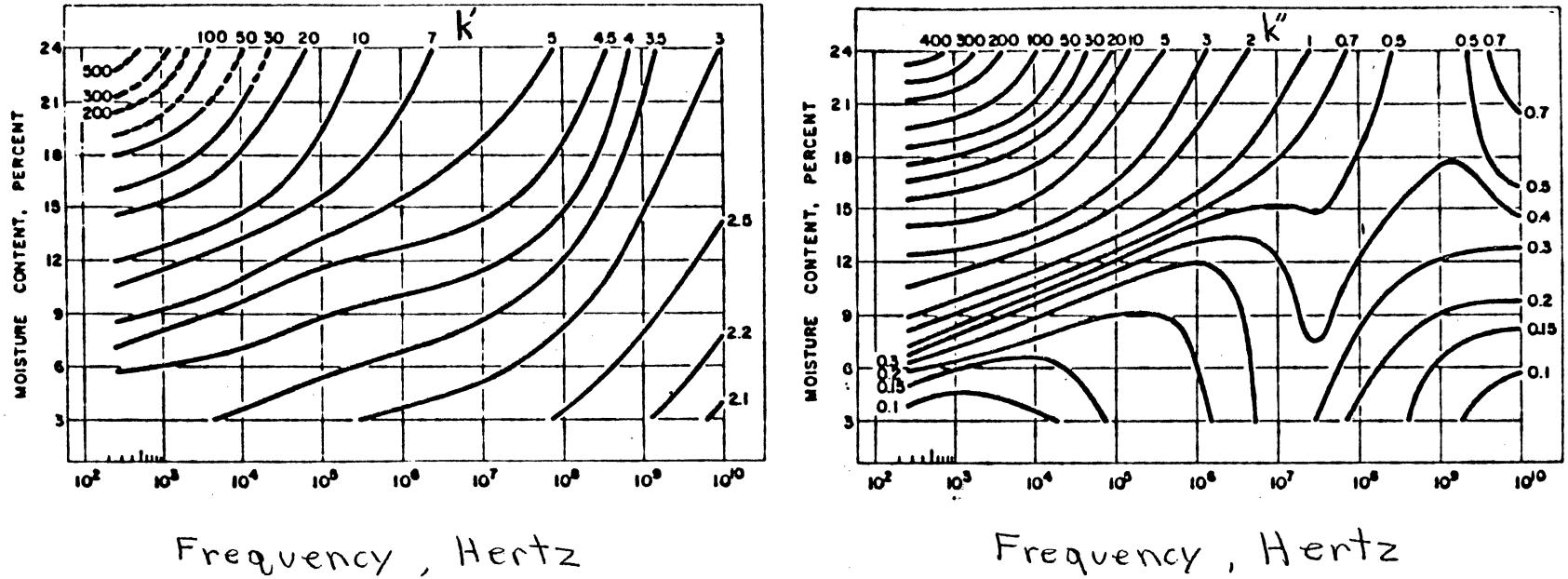

Figure 1. Contour Plots of k' and k" for Hard Red Winter Wheat as a Function of Frequency and Wet-Basis Moisture Content [2].

dielectric medium is free space, and the only electric charge present is distributed as a surface charge density over the two oppositely and equally charged conductors, the capacitance of the system becomes:

$$C_o = Q / V \qquad (1\text{-}2\text{-}6)$$

where Q is the total charge, and V is the potential difference between the conductors. If the volume of the capacitance cell is filled with a dielectric material other than free space, the capacitance increases linearly:

$$C = C_o \varepsilon'/\varepsilon_o = C_o k' \qquad (1\text{-}2\text{-}7)$$

where k' is the relative dielectric constant of the new material. Since there is a one-to-one correspondence between k' and C, either one can be calculated through the relationship:

$$k' = C/C_o \ . \qquad (1\text{-}2\text{-}8)$$

Physical capacitors exhibit energy losses, and this phenomenon can be represented by a resistor, R; it represents all the energy dissipative processes in the dielectric material.

As a measure of the energy storage efficiency of a capacitor, a quality factor, Q, is defined as the ratio of the maximum energy stored per cycle to the energy dissipated per cycle. For a parallel RC circuit, Q becomes:

$$Q = \tfrac{1}{2}CV^2 \ / \ (\tfrac{1}{2}V^2 \ / \ \omega R) = \omega RC \ . \qquad (1\text{-}2\text{-}9)$$

The quality factor can also be expressed in terms of k' and k". Neglecting end effects of a paralled plate

capacitor, and assuming a uniform electric field, E,

$$E = V / d \quad \text{volts/meter} \tag{1-2-10}$$

where V is the potential difference, and d is the distance between plates. An alternate expression for Q can be derived using the current density relationships. The capacitor draws a charging current, I_C:

$$I_C = dQ/dt = j\omega CV = j\omega V\varepsilon'A/d = j\omega E\varepsilon'A \tag{1-2-11}$$

and its associated current density is:

$$J_C = I_C/A = j\omega E\varepsilon' \text{ Ampere/meter}^2 \tag{1-2-12}$$

Similarly, the current density in the resistor is:

$$J_R = E\sigma = E\omega\varepsilon'' \text{ Ampere/meter}^2 \tag{1-2-13}$$

where ω is the radian frequency. Figure 3 shows the phase relationship between these two quantities, J_C and J_R. The ratio of J_C to J_R defines a loss tangent which is also used as a definition of the quality factor

$$Q \equiv \tan\Theta = E\varepsilon'/E\varepsilon'' = \varepsilon'/\varepsilon'' = k'/k'' \ . \tag{1-2-14}$$

Equation (1-2-14) applies equally to all capacitance cell geometries, and it shows that k' and k" are not independent.

It is now obvious that k' and k" can be indirectly calculated through equations (1-2-8) and 1-2-14), once the values for C and Q have been measured. Although these equations convey an underlying approach to calculating k' and k", improvements can be made by considering the extraneous capacitances which affect the measured value. The corrected equation for the test cell's capacitance should include: the edge capacitance (i.e. any capacitance

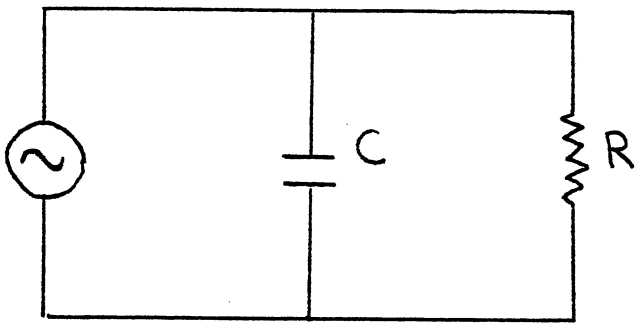

Figure 2. Parallel RC Equivalent Circuit of a Capacitor Having a Lossy Dielectric.

$J_c = j\omega E \epsilon'$ $\qquad$ $J_s = (\epsilon'' + j\epsilon')\omega E$

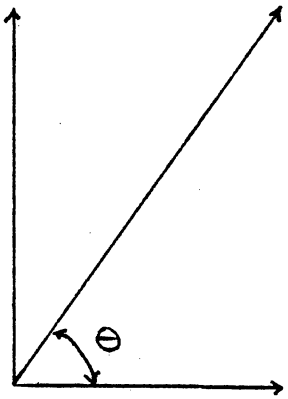

$J_L = \omega E \epsilon''$

$\theta = \tan^{-1}(\epsilon'/\epsilon'')$

Figure 3. Time Phase Relationship Between Charging Current Density and the Loss Current Density.

due to flux lines that do not penetrate the test medium) and the ground or lead capacitance. A thorough discussion on these residual impedances is given in Chapter II of Von Hipple [3].

Since the intention of this research is the evaluation of a sensor, and not necessarily to attempt to measure the dielectric properties of wheat, the values used in this analysis are taken from published data. It should be noted, however, that these values are only approximations to the actual ones for the wheat used for testing purposes. Figure 4(a) shows several plots of constant moisture content curves on a k' versus frequency graph. This figure not only provides general values of k', but it also provides insights as to how k' varies with different moisture contents at fixed frequency. Similarly, Figure 4(b) shows several plots of constant moisture content curves on a k" versus frequency graph [4].

1.3 Grain Bulk Density and Permittivity Relationships

In addition to moisture content, variations in the permittivity can also be attributed to variations in the bulk density of the grain sample, and two basic perspectives in dealing with bulk density are of interest: variations in bulk density for a given lot of grain; and variations in bulk density among different lots of the same variety of grain. The latter case is much more complicated

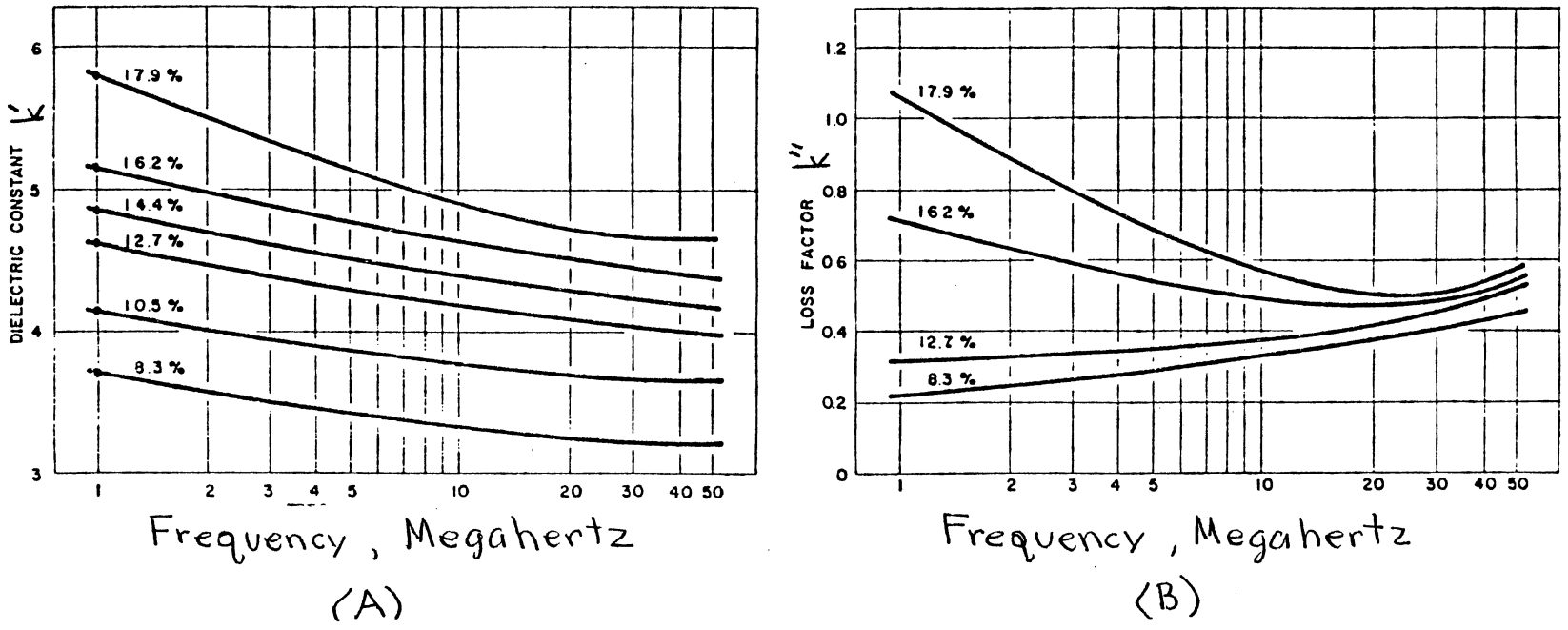

Figure 4. Contour Plots of Constant Moisture Content for Hard Red Winter Wheat as Functions of k', k", and Frequency [2] .

to analyze since the characteristics of grain vary considerably between lots. This nonhomogenity can be attributed to soil and climatic conditions [2]. Cases involving only a single lot lend themselves to simple models relating bulk and kernel density to permittivity.

Linear models can be constructed that relate the square root of the dielectric constant, k' , to the bulk density, p_b, of grain. The linear equation is of the form

$$(k')^{\frac{1}{2}} = a\, p_b + b \,, \qquad (1\text{-}3\text{-}1)$$

and the constants 'a' and 'b' are calculated through curve fitting techniques using $(k')^{\frac{1}{2}}$ versus p_b plots. These plots were constructed from known moisture content samples at selected frequencies. It is evident that the bulk density of grain does affect the dielectric constant of the grain sample. Figure 5 shows a linear relationship between $(k')^{\frac{1}{2}}$ and p_b for hard red winter wheat [2].

Since electrical capacitance type moisture meters depend on the dielectric properties of grain, it is advantageous to minimize the fluctuations in additional factors, other than moisture content, which affect these properties. Variations in bulk density affect the dielectric constant as seen in equation (1-3-1) and Figure 5, and commercial moisture meters control the variations by weighing the grain sample to ensure consistancy in the sample mass. Typically, this is done automatically by built-in hopper scales.

Frequency and temperature are two additional factors

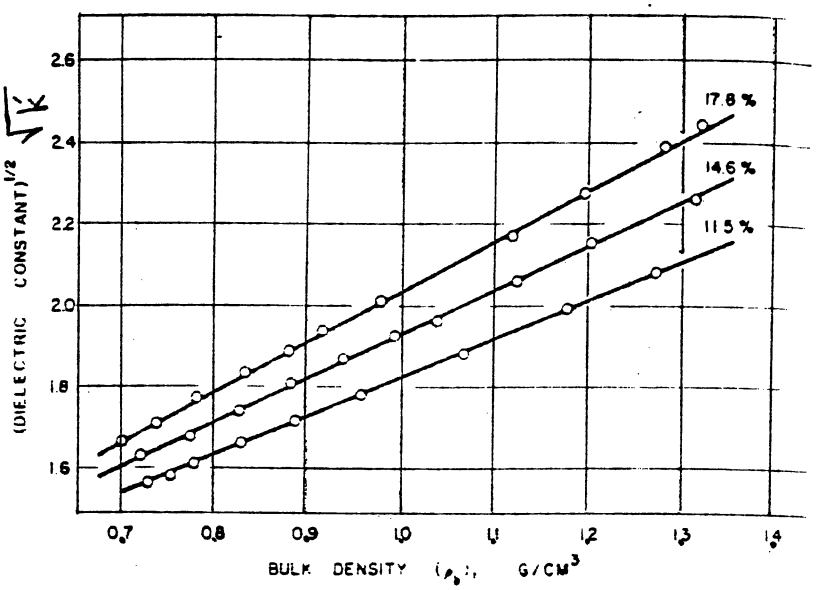

Linear relationships for the square root of the dielectric constant at 9.4 GHz and bulk density of hard red winter wheat at indicated wet-basis moisture contents. Straight lines for experimental points: 17.8 percent, $\sqrt{\varepsilon'} = 0.814 + 1.223\,\rho_b$; 14.6 percent, $\sqrt{\varepsilon'} = 0.850 + 1.079\,\rho_b$; 11.5 percent, $\sqrt{\varepsilon'} = 0.874 + 0.950\,\rho_b$. For theoretical zero-bulk-density intercept, $\sqrt{\varepsilon'}$ should = 1.0

Figure 5. Linear Relationship for the Square Root of the Dielectric Constant and Bulk Density of Hard Red Winter Wheat [2].

which should be regulated to enhance the performance of the moisture meter. Commercial moisture meters usually employ an automatic temperature correction system. Oscillator frequency stability is also crucial since ε' is positively correlated with frequency for a given moisture content [2].

1.4 Electrical Capacitance Moisture Meter

Intended for agricultural purposes, an early design example of incorporating the capacitance cell and the moisture dependent dielectric properties of grain into a moisture meter is presented in a paper by Matthews (1962) [4]. He discusses the design criteria and evaluation procedures used in developing a portable capacitance cell electric moisture meter, and important items concerning the moisture sensor are recounted in this section.

The overall performance of a moisture meter is affected by the ensemble of individual performances of components making up the entire system. In order to enhance the moisture meter's performance, it is advantageous to select the sensor's geometry and/or its physical dimensions such that it has an acceptably small error. Matthews [4] evaluates two capacitance cell geometries for use in a portable moisture meter.

The two cell geometries considered by Matthews [4] were the parallel-rectangular plate and the concentric-cylindrical electrode configurations. Preconditioned moisture content samples of hard red winter wheat were used

in one series of tests. The objective of the test was to observe how geometry and/or volume affected the sensor's sensitivity to changes in moisture content. After adhering to a consistent filling and emptying procedure, the results of this test revealed that the sample variances for the cylindrical cells were consecutively higher as compared to sample variances for the rectangular cells. This increase can be attributed to the influences of the non-uniform electric field associated with the cylindrical cell. The electric flux density in the cylindrical cell is greatest near the inner cylinder, thus the random settling of grain around the inner conductor has significant effects on the sample variance. This becomes more noticeable as the circumference of the inner conductor decreases. When comparing the sample variances between similar geometries of different volumes, it tends to decrease slightly as the volume increases. This decrease is due to the fact that the sample size increases proportionately with volume; thus it is expected that the sample variance will decrease. Matthews [4] points out that the ultimate limitation to a moisture meter's precision is determined by the random variability of the grain bulk density, primarily caused by inconsistent filling and/or settling of grain; in addition, variations in bulk density also exist due to natural and biological influences. Attempts to minimize this error are made by accurately weighing the sample and consistent filling of the test cell. Additional enhancements can be

accomplished by implementing a temperature compensation element into the circuit design. Regarding capacitance cell design, it was suggested that either one of the geometries evaluated would suffice. Matthews [4] chose to use a cell of approximately 25-30 cm^3 volume fitted with a parallel plate electrode in the construction of his portable moisture meter, and the cell's capacitance was approximately in the picofarad range.

Although considerable emphasis is placed on handling the problems associated with bulk density, sufficient thought should also be given to the design of the sensor. Several considerations are now summarized concerning capacitance cell design.

(1) The test cell's geometry should have characteristics that enable it to minimize external influences affecting its electrical characteristics, and the test cell must also have a high enough capacitance so that extraneous capacitive effects are negligible or easily compensated.

(2) The dimensions of the electrodes must be properly chosen to minimize the effects of the nonuniform grains. If the electrodes are much longer than the longest dimension of a single grain, the effects of grain orientation are insignificant due to their assumed random orientation.

(3) The test cell's volume is not too critical as long as it is permissible to assume that the effects caused

by the random distribution of the grain kernels essentially cancel. The electrodes should be spaced so that the grain is able to flow freely in and out of the cell. The critical concern, however, is the variability in filling the test cell; this leads to variations in the bulk density. Therefore, it is essential to exercise consistency when filling the test cell.

(4) The difficulties inherent in the last three statements are compounded when designing a nonintrusive moisture sensor. This can be attributed to the nature of the electric field of these sensors. The inherent problem is that the grain sample is subjected to the weaker fringe-field rather than the primary field which is usually much more predominant. A detailed discussion of the fringe field capacitance cell is given in section 2.2.

1.5 Comments

Out of the three electrical properties of grain previously discussed, the dielectric constant k' was found to be influenced the most by moisture content, and a positive correlation exists between k' and moisture content. Nelson [2] concludes his study by stating that the best single dielectric property to use as a moisture content indicator is k' since the inherent dependency of k', on moisture was observed to be the highest among the dielectric properties of grain. Variations in grain density must also be considered when performing moisture measurements, and

corrections are typically employed to compensate for this variation.

1.6 Problem Statement

The objective of this thesis research is to investigate the use of a microstrip capacitor for grain moisture measurement. Figures 6(a) and 6(b) show simplified sketches of the microstrip configuration investigated as the moisture sensor in this study. The premise in choosing this geometry was primarily to have a nonintrusive moisture sensor, that is, the grain's moisture content is measured as the grain comes in contact with the sensor. Intrusive moisture measurement is typically understood to be the operation where samples of the grain are removed from the lot, and inserted into a closed capacitance cell. The capacitance cell will function as the sensor in an electric moisture meter. The investigation will include both theoretical and experimental work, leading to a discussion of the differences that are expected to be present.

The mathematical model of the sensor will be based on a computer-implemented approximation of the electrostatic potential field map in close proximity to the microstrip conductor. The field map is generated by using a finite difference approximation to partial differential equations for problems having open boundaries. The following assumptions will clarify the meaning of the term 'infinity'

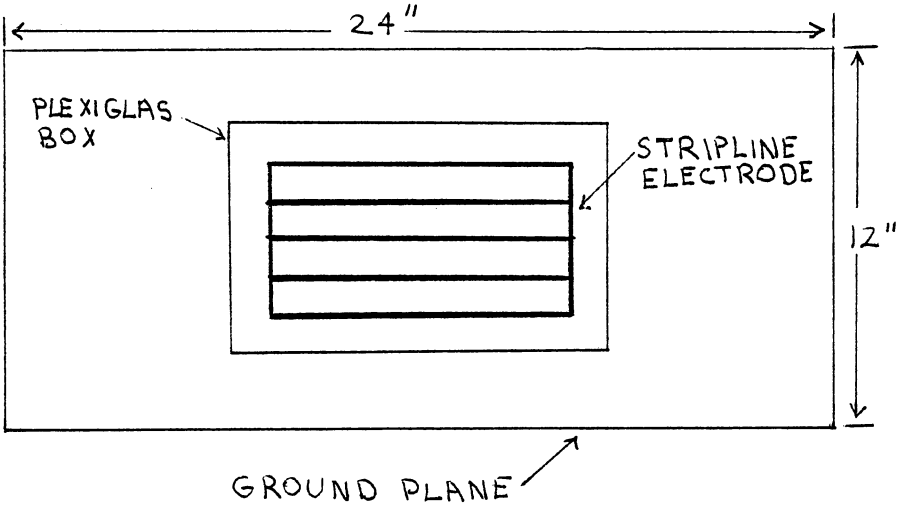

(A) Top View of Test Apparatus

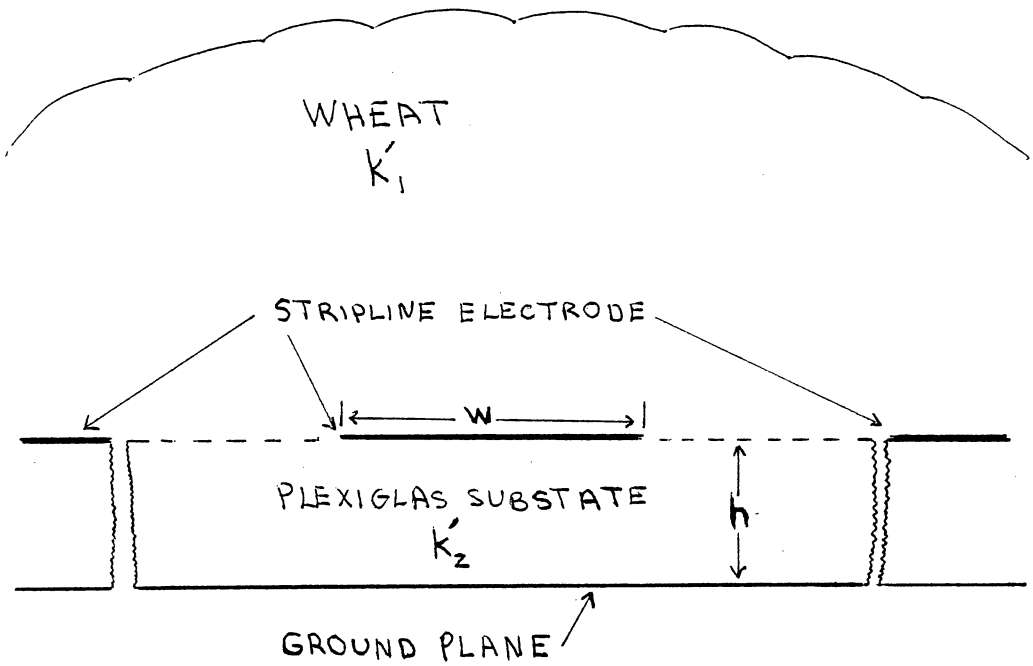

(B) Width-Wise View of Microstrip

Figure 6. Sketch of Grain Moisture Sensor

in the previous description: referring to Figure 6(a), the ground plane is considered to be a much larger surface area than the microstrip electrode; the depth of wheat is much larger than the distance separating the electrode from the ground plane, and the length of the microstrip is much larger than the width of the microstrip.

Two applications of the field map are: (i) it can be used to approximate the characteristic capacitance of a microstrip configuration for given dimensions and dielectric constants, and (ii) it can function as an indicator of the change in the cell's capacitance due to changes in the dielectric constant.

The scope of this research will consist of developing an idealized model and limited testing of a prototype test cell. Results of this research are expected to provide insights into the behavior of the electric field near a microstrip conductor and the application of this configuration as a sensor in grain moisture measurements.

1.7 Outline of the Study Approach

Development of the idealized model will be based on several fundamental assumptions. These assumptions are termed fundamental since they are based on proven studies and/or theory governing electromagnetism. The primary assumption is that the sample volume of grain is considered to be a linear homogeneous isotropic dielectric medium having a dielectric constant, k' and a loss factor, k".

Further assumptions will be introduced later as appropriate.

Chapter 2 presents the technique used in this research to calculate the characteristic capacitance of a microstrip configuration. This technique is based on a numerical relaxation method for boundary value problems having open boundaries. Two possible applications of the characteristic capacitance are: (i) provide a basis for the evaluation of microstrip geometries as moisture sensors, (ii) and provide approximations for the capacitance of the microstrip.

Chapter 3 deals with the construction and testing of the prototype microstrip capacitor cell. The tests are conducted to evaluate the validity of the computer model. The chapter conludes by summarizing the experimental investigations using the microstrip sensor and a vector impedance meter to detect changes in moisture content of wheat.

Chapter 4 presents a summary of the work and the conclusions drawn from it. Suggestions are made concerning further research on the design and implementation of microstrip configurations as moisture meters.

CHAPTER II

ELECTRICAL CAPACITANCE-TYPE MOISTURE SENSORS

2.1 Introduction

It has been shown empirically that the dielectric properties of grain are reliable indicators of the grain's moisture content. The dielectric constant, k', is the single best indicator of moisture content since its correlation with moisture content is the highest of all the dielectric properties. The preeminent characteristic of k' leads to the employment of a capacitance cell as the moisture sensor in electric moisture meters. This chapter is primarily concerned with the design and evaluation of the moisture sensor.

2.2 Fringe Field Capacitance Cell

The premise in using a nonintrusive moisture sensor is to allow the grain to flow freely through the sensor without any obstructions. This technique permits, in addition to its speed, a relatively larger number of moisture measurements, as compared to the slower technique of having to remove samples in order to perform the tests. It is expected that a larger number of measurements would

improve the accuracy in estimating the moisture content. Having a moisture measurement on an almost continuous basis, a closed-loop moisture control system for example, would enhance the quality control of moisture content.

In studying a complex problem, one typically begins by breaking it down into subsections according to difficulty. This study will be concerned with analyzing and testing the simple case where the grain sample is stationary. The challenges associated with flowing grain will be left for further research. The remainder of this chapter discusses an analytical technique used to compare the sensitivities of two microstrip capacitance cells. It is hoped that one of the two cells will exhibit higher sensitivity to changes in the grain's moisture content. Sensitivity will be discussed further in the next section.

2.3 Analytical Discussion of the Microstrip Moisture Sensor

In order to have a quantitative evaluation for different microstrip dimensions (i.e. various width to height ratios), a sensitivity factor can be defined which incorporates the characteristic capacitance of the microstrip. The microstrip cell geometry evaluated in this research is shown in Figure 7. The two proposed cells evaluated in this research differ only in the distance separating the electrode and the ground plane. The electrode and ground plane are separated by a sheet of

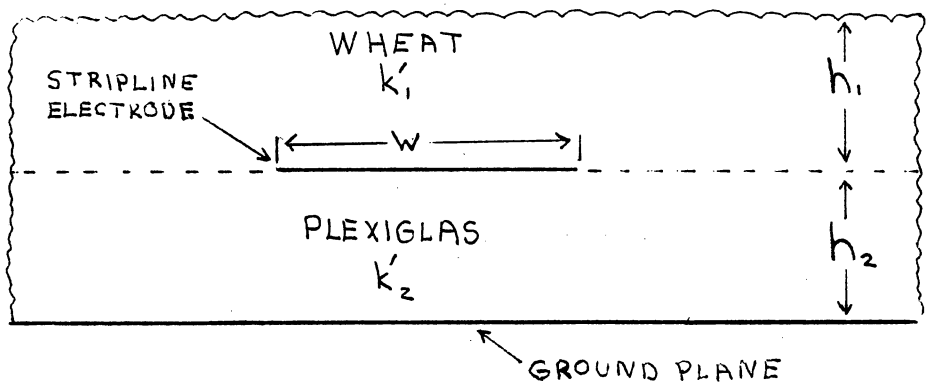

Figure 7. Cross Sectional View of Microstrip Capacitance Cell Geometries ($h_1 \gg h_2$ and $L \gg h_2$).

plexiglas. The second cell is simply constructed from the first cell by placing an additional sheet of plexiglas between the conductor and the ground plane.

To develop a theoretical design criterion, a sensitivity factor, SF, is next established. Electrical capacitance is a geometric phenomenon dependent upon the dielectric medium confined within the capacitor. Assuming an ideal capacitor (i.e. negligible fringe-field), the capacitance proportionally changes as the dielectric constant of the medium changes.

$$C'_p = k' C_p \qquad (2\text{-}3\text{-}1)$$

where C_p is the cell's capacitance when the medium is free-space, and C'_p is the cell's capacitance when it's volume is filled with a dielectric medium having a dielectric constant of k'. Note that equation (2-3-1) is a general expression which is applicable to capacitors involving a single dielectric material. When dealing with the capacitance cell geometry proposed in this study, the cell's capacitance is dependent on two dielectric materials: the dielectric constant of the material above the microstrip and the dielectric constant of the material separating the microstrip and the ground plane. Since the dielectric properties of the plexiglas substrate are assumed to remain constant, the cell's capacitance, C_p, can be expressed as a function of a single variable, namely k'_1. This is desirable, because the premise in using capacitance-type moisture meters is to sense the grain's

moisture content by measuring the change in the cell's capacitance caused by a change in the cell's capacitance by a change in k'_1. Using the previous assumption, equation (2-3-1) is modified by incorporating a sensitivity factor, SF.

$$C'_p = (SF)\ k'_1\ C_p \qquad (2\text{-}3\text{-}2)$$

A qualitative interpretation of equation (2-3-2) can be stated: If the plexiglas substrate were replaced by wheat so that the cell's volume is filled with a single dielectric material, namely wheat, the SF would be equal to unity. Therefore, the SF has a maximum value of 1.

Solving equation (2-3-2) for the SF, the SF becomes:

$$SF = C'_p\ /\ (C_p\ k'_1) \qquad (2\text{-}3\text{-}3)$$

The capacitances C_p and C'_p can be further divided in terms of the capacitances of the upper and lower regions:

$$C_p = C_1 + C_2 \qquad (2\text{-}3\text{-}4)$$

$$C'_p = C'_1 + C'_2 \qquad (2\text{-}3\text{-}5)$$

where the subscripts 1 and 2 denote the upper and lower region, respectively. Figure 8 shows a physical interpretation of C_1 and C_2. Since the dielectric properties of the plexiglas substrate are assumed not to change, the sensitivity factor becomes a function of k'_1; Using equations (2-3-4) and (2-3-5) in equation (2-3-3), the SF becomes:

$$SF(k'_1) = (C'_1+C'_2)/[(C_1+C_2)k'_1] \qquad (2\text{-}3\text{-}6)$$

When employing a microstrip configuration as a

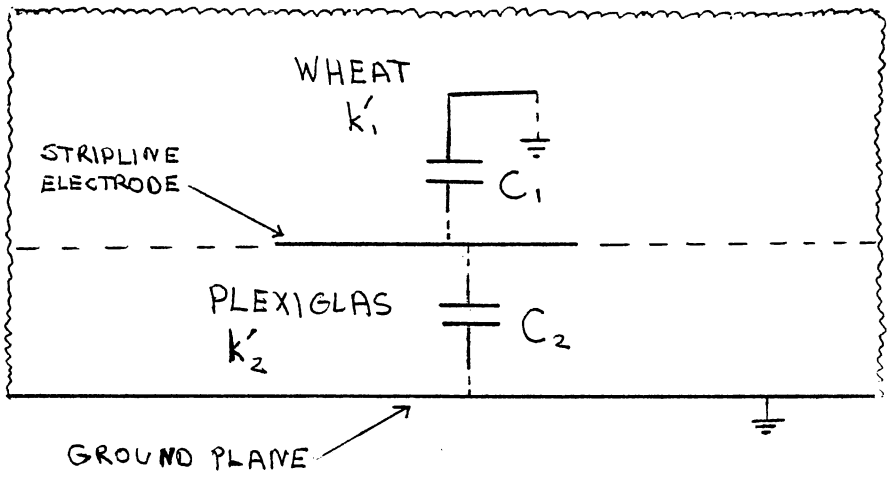

(A) Physical Interpretation of Capacitors C_1 and C_2.

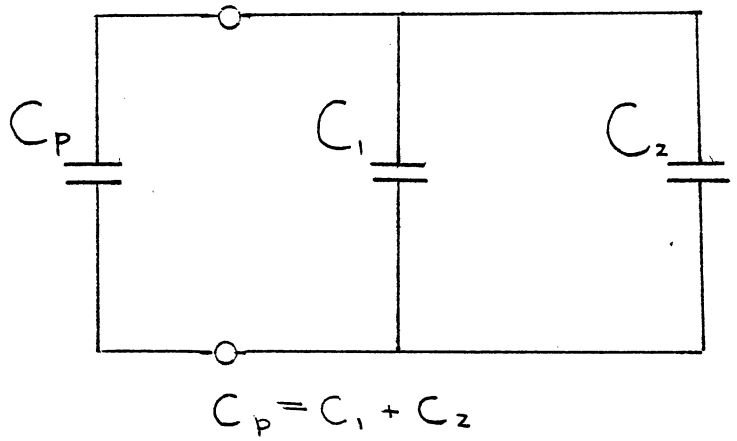

(B) Equivalent Parallel Circuit Model.

Figure 8. Representations of Microstrip Capacitance.

moisture sensor, it is unfortunate that only a small percentage of the total electric flux density is confined within the dielectric material of interest, namely wheat. The objective of the following section and its subsections is to present the technique used in this research to approximate the values for the capacitances, C'_p and C_p in equation (2-3-4). Sensitivity factors for the two proposed cell configurations are calculated in section 2.4. The last section discusses the differences in the sensitivity factors of the two test cells, thus it is expected that a preference to one test cell over the other can be made.

2.3.1 Approximating the Characteristic Capacitance of a Microstrip

The capacitance of a two-conductor system is defined as the ratio of the total charge to be transferred from one to the other to the potential difference between conductors

$$C = Q / V \qquad (2\text{-}3\text{-}7)$$

In general terms, the charge, Q, can be expressed as a surface integral over the positive conductor:

$$Q = \int \varepsilon \, \bar{E} \cdot d\bar{S} \qquad (2\text{-}3\text{-}8)$$

and the potential difference, V, can be expressed as a line integral along a path from the negative to the positive conductor,

$$V = - \int \bar{E} \cdot d\bar{L} \qquad (2\text{-}3\text{-}9)$$

Equation (2-3-7) can now be expressed in general terms using equations (2-3-8) and (2-3-9)

$$C = \frac{\int \varepsilon \, \bar{E} \cdot d\bar{S}}{-\int \bar{E} \cdot d\bar{L}} \qquad (2\text{-}3\text{-}10)$$

If a closed-form expression of the electric field intensity, E, exists, the capacitance can be readily calculated by using equation (2-3-10). However, many instances occur in practice when a closed-form expression of E is much too complicated to find. Consequently, numerical techniques have been developed which can be easily realized on a digital computer.

The technique used in this study to approximate the potential field map in close proximity to the strip line is a successive overrelaxation (SOR) of finite difference approximations to partial differential equations. Numerical relaxation techniques have been well developed, and an informative paper by Wexler [5] reviews some of the computational techniques used to solve electromagnetic field problems. Papers by Green [6] and Judd (et.al.) [7] discuss numerical solutions of transmission-line problems, and both papers present numerical results which can be used for comparison of the SOR technique used in this study. Refering to Figure 7, it is apparent that this is an unbounded problem. The electric field is not confined within a finite region between conductors. Therefore, it

is necessary to assume that the electric field approaches zero at infinity; this is one of the boundary conditions that must be incorporated. A paper by Sandy and Sage [8] describes a method for dealing with problems having boundaries at infinity, and the SOR technique used in this research comes from this reference.

The SOR technique for approximating mathematical operations and functions is based on the assumption that if the domain of a continuous operation is broken into a set of discrete points, and the discretized operation performed on this discrete point set, this discretized approximation of the operation becomes increasingly more accurate as the distance between points becomes sufficiently small [5]. In approximating the electric field map, the operation to be discretized is Laplace's equation

$$\nabla^2 \varphi = 0 \qquad (2\text{-}3\text{-}11)$$

In two dimensional Cartesian coordinates, equation (2-3-11) becomes

$$\nabla^2 \varphi = \partial^2\varphi / \partial^2 x + \partial^2\varphi / \partial^2 y = 0 \qquad (2\text{-}3\text{-}12)$$

To determine the discretization of a derivative, consider the following Taylor's expansion of a continuous function, f, at (x+h):

$$f(x+h) = f(x)+hf'(x)+\tfrac{1}{2}h^2f''(x)+1/6h^3f'''(x)+... \qquad (2\text{-}3\text{-}13)$$

and at (x-h):

$$f(x-h) = f(x)-hf'(x)+\tfrac{1}{2}h^2f''(x)-1/6h^3f'''(x)+... \qquad (2\text{-}3\text{-}14)$$

Next, subtracting equation (2-3-13) from equation (2-3-14)

and rearranging gives:

$$f'(x) = [f(x+h)-f(x-h)] / 2h + O(h^2) \qquad (2\text{-}3\text{-}15)$$

where $O(h^2)$ represents an error term of the order h^2 for this approximation; h^2 is considered to be almost the sole contributor to the error term. Equation (2-3-15) is the central difference formula for the first derivative. This relationship is shown in Figure 9. The second derivative can also be calculated by using the same three points as before: (x-h), (x), and (x+h) . Using the (x+h/2) and (x-h/2) as the center points, the difference equations become:

$$f'(x+\tfrac{1}{2}h) = [f(x+h)-f(x)] / h \qquad (2\text{-}3\text{-}16)$$

and

$$f'(x-\tfrac{1}{2}h) = [f(x)-f(x-h)] / h \qquad (2\text{-}3\text{-}17)$$

The second derivative at x can be calculated as

$$f''(x) = [f'(x+\tfrac{1}{2}h)-f'(x-\tfrac{1}{2}h)] / h \qquad (2\text{-}3\text{-}18)$$

Substituting in for f'(x+h/2) and f'(x-h/2), equation (2-3-18) becomes

$$f''(x) = [f(x+h)-2f(x)+f(x-h)] / h^2 \qquad (2\text{-}3\text{-}19)$$

where the error term term is still of the order h^2. Equation (2-3-19) is next applied to the Laplacian operator, and the discretized version of equation (2-3-12) becomes :

$$\nabla^2\varphi = [\varphi_{i,j+1} + \varphi_{i-1,j} + \varphi_{i,j+1} + \varphi_{i+1,j} - 4\varphi_{i,j}]/h^2 \qquad (2\text{-}3\text{-}20)$$

Figure 10 shows the five point finite difference operator for the case of equispaced points.

Setting equation (2-3-20) equal to zero gives a

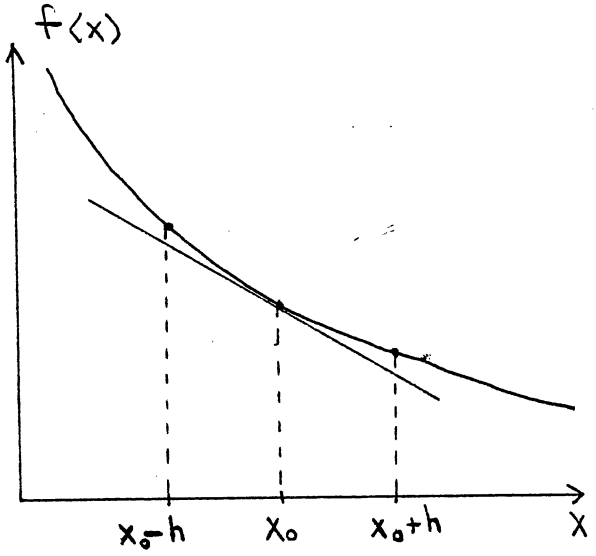

Figure 9. Central Difference Equation.

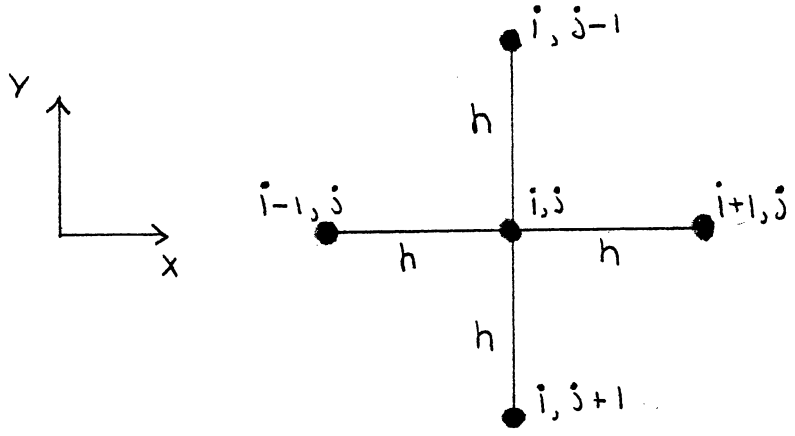

Figure 10. Five Point Finite Difference Operator.

discretized version of Laplace's equation for a two dimensional Cartesian coordinate system.

$$\varphi_{i,j+1} + \varphi_{i,j-1} + \varphi_{i+1,j} + \varphi_{i-1,j} - 4\varphi_{i,j} = 0 \qquad (2\text{-}3\text{-}21)$$

Equation (2-3-21) is the case when it is assumed that there are no free-charges in the dielectric medium. Rearranging equation (2-3-21), and supplying reference to the iteration stage, k, yields the following nodal expression:

$$\varphi_{i,j}(k) = [\varphi_{i,j+1}(k)+\varphi_{i,j-1}(k)+\varphi_{i+1,j}(k)+\varphi_{i-1,j}(k)]/4 \qquad (2\text{-}3\text{-}22)$$

This set of simultaneous equations can be solved through iterative techniques.

When using numerical techniques to solve boundary value problems that have boundaries extending to infinity, a particular difficulty arises in dealing with this condition. The typical solution has been to impose a boundary condition of constant potential at a finite distance from the microstrip. In a paper by Judd et-al. [7], it was found that satisfactory results are achievable when this distance from the boundary is taken to be 10 times the distance separating the mictrostrip from the ground plane. The disadvantage in this approach is that a large number of lattice points are required to accurately approximate the potential field in close proximity to the electrode. An alternative approach given by Sandy and Sage [8] suggests that an artificial boundary, much closer to the microstrip, can be defined. Since this boundary will not be at a constant potential, its value must also be

determined by incorporating a boundary relaxation scheme along with a conventional technique for relaxing the interior points. Figure 11 shows a sketch of this arrangement. The following steps outline the procedure described by Sandy and Sage [8] :

(1) Define a fictitious boundary, S, near the microstrip, and assign it an initial potential of approximately one half that of the potential difference between the electrode and ground plane.

(2) Use conventional relaxation techniques to determine the potential inside the given region.

(3) Approximate the potentials on the boundary by assuming that the microstrip and the dielectric interface can be replaced by a horizontal row of discrete line charges, and the ground plane is replaced by assuming respective image charges. The potential at a point on the boundary S can be calculated by integrating the Poisson's equation.

$$\nabla^2 \varphi = - \rho / \varepsilon \qquad (2\text{-}3\text{-}23)$$

The line charge density, ρ_o, normal to the page is next calculated using the five-point discretized approximation to the Poisson's equation.

$$\rho_o = - \varepsilon (\varphi + \varphi + \varphi + \varphi - 4\varphi)/h^2 \qquad (2\text{-}3\text{-}24)$$

The potential for a nodal point on S is calculated by summing the contributions of ρ_o.

$$\varphi_S = (1/2\pi\varepsilon) \sum_{i,j} \rho_o(i,j) \quad \ln(R/R') \quad \text{(volts)} \qquad (2\text{-}3\text{-}25)$$

where R is the distance from the line charge, $_o$, to the

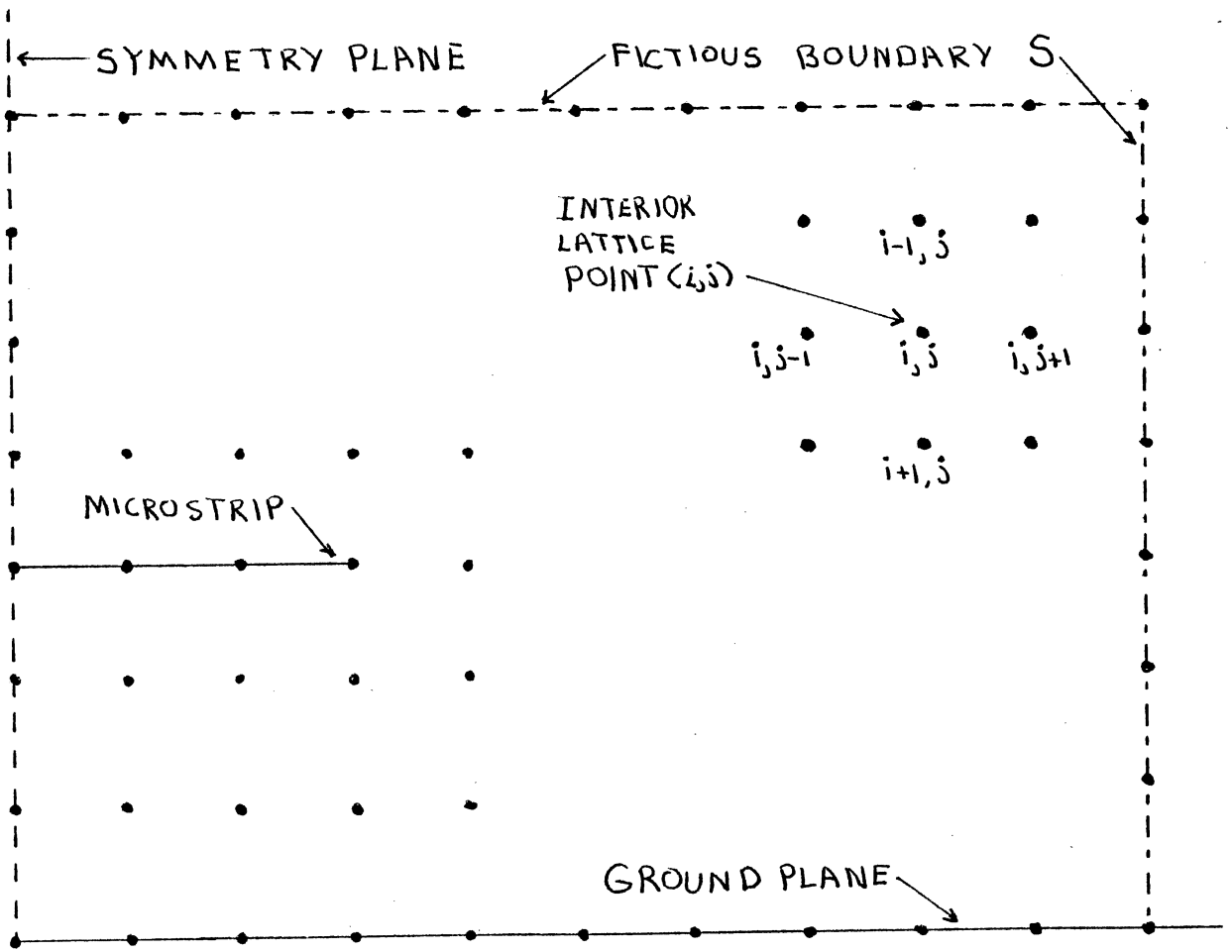

Figure 11. Potential Field Map for the Microstrip Configuration.

point on the surface, S, and R' is the distance from its image to S. Using equation (2-3-25), the new values for the node potentials on S are next calculated by summing the contributions generated from each point charge and its image. If this new potential is significantly different from its old value, the old value is replaced with the new one. Otherwise, the potential remains the same. If it was required to change any one of the nodal values on S, the process has not converged, and step (2) is repeated using the new boundary potential. Sandy and Sage [8] offers an example of this procedure and shows that it does not conflict with the uniqueness theorem.

2.3.2 Liebmann's Iteration Method

Rather than relaxing all the lattice points in one step, as is done in conventional relaxation techniques, Liebmann's method immediately relaxes the potential at a particular point before moving the process to the next sequential point. If the absolute value of the residual, calculated at a particular point, is greater than a predetermined minimum residual value, R_0, the potential at that point is augmented to a new value. This new potential is determined by adding the old potential to the product of the residual and an overrelaxation factor. If the residual is within limits of the minimum residual, the potential is unaltered. The following steps outline this process [9].

(1) The boundary potentials are first specified.

Typically, in a two conductor system, one conductor is assigned a constant potential, φ_o, and the other conductor, or boundary condition where the electric field is allowed to terminate, is assigned a potential of zero volts. The interior points, which are to be determined in the next step, are given arbitrary values between φ_o and zero. The procedure used in this thesis modifies this step; the potential on the boundary S is relaxed using the method outlined in the previous section.

(2) The iterative cycle proceeds usually in a left to right and top to bottom fashion, sequentially relaxing each interior lattice point. For example, the residual at point (i,j) shown in Figure 11 is calculated by using equation (2-3-22).

$$R_{i,j} = \varphi_{i,j} - [\varphi_{i+1,j} + \varphi_{i-1,j} + \varphi_{i,j+1} + \varphi_{i,j-1}](\alpha/4) \qquad (2\text{-}3\text{-}26)$$

where α is the acceleration factor, and the subscripts 'i' and 'j' indicate the position of a lattice point.

(a) If the absolute value of $R_{i,j}$ is greater than R_0, $\varphi_{i,j}$ is 'over-relaxed' to a new value.

$$\varphi_{i,j} = \varphi_{i,j} - R_{i,j} \qquad (2\text{-}3\text{-}27)$$

(b) If the absolute value of $R_{i,j}$ is less than R_0, Laplace's equation is 'satisfied' for that lattice point, and $\varphi_{i,j}$ is not altered.

(3) Continue with step (2) until all the residuals have been relaxed to within R_0, or terminate the process when the number of iterations has exceeded its maximum

value.

It can be proven that Liebmann's method converges for closed boundary problems [9]. Additionally, an optimum overrelaxation factor, α_{opt}, can be found thus enhancing the speed of convergence. Applicable to the class of 'elliptic' partial differential equation, including Poisson's and Laplace's, an optimum overrelaxation factor can be estimated from the following equations [10].

$$\alpha_{opt} = 4/[2 + (4 - C^2)^{\frac{1}{2}}] \qquad (2\text{-}3\text{-}28)$$

with

$$C = [\cos(\pi/p) + \cos(\pi/q)] \qquad (2\text{-}3\text{-}29)$$

where p and q are the number of points defining the rectangular region.

2.3.3 Accuracy of a Numerical Solution

Once the numerical solution has been found, the next concern deals with determining the accuracy of the results. Ideally, the error in the numerical solution approaches zero in the limit as the number of points increase to infinity (ie. the mesh covering the region becomes infinitesimally small), and the minimum residual is set to zero. Since the computer only has a finite amount of memory space, the number of lattice points and a value for the minimum residual are chosen within practical limits.

Scarborough [11] discusses an inherent error term used to compare the relative error between two approximations of the solution at a given nodal point. Recall that the error

term in the approximation to Laplace's equation (2-3-21) was assumed to be of the order h^2, if terms of higher powers of h^2 are neglected. An inherent error term can be expressed as

$$E = ch^2 \qquad (2\text{-}3\text{-}30)$$

where c is some arbitrary constant. A 'truer' solution of V becomes

$$V^* = V + ch^2$$
$$= V + E \qquad (2\text{-}3\text{-}31)$$

Scarborough [11] next considers two grid sizes, h_1 and h_2. Where

$$h_2 = \tfrac{1}{2} h_1 \qquad (2\text{-}3\text{-}32)$$

Inserting h_1 and h_2 into equations (2-3-31) and (2-3-30), the respective equations become:

$$E_1 = ch^2{}_1 \qquad (2\text{-}3\text{-}33)$$

$$E_2 = ch^2{}_1 \qquad (2\text{-}3\text{-}34)$$

$$V^* = V_1 + ch_1{}^2 \qquad (2\text{-}3\text{-}35)$$

$$V^* = V_2 + ch_2{}^2 \qquad (2\text{-}5\text{-}36)$$

Replacing $h_2{}^2$ in equation (2-3-34) with equation (2-3-32), and solving for $h_1{}^2$ in this equation and equation (2-3-33), a relationship between E_1 and E_2 is given.

$$E_2 = 1/4\ E_1 \qquad (2\text{-}3\text{-}37)$$

Equation (2-3-37) states that the error in the approximation of V^* for the first grid size, h_1, can be reduced by a factor of one-fourth, if a new grid size equal to one-half of the original grid is used. Another useful relationship can be found by setting equation (2-3-35)

equal to equation (2-3-36), and solving for E_2.

$$ch_2^2 = c_1^2 + (V_1 - V_2)$$

using $E_2 = ch_2^2$

and $E_1 = ch_1^2 = 4E_2$

the final result is

$$E_2 = (1/3)\ (V_2 - V_1) \qquad (2\text{-}3\text{-}38)$$

where the subscripts 1 and 2 denote the calculations using h_1 and h_2, respectively.

The number of lattice points needed to achieve the desired tolerance specified by a prescribed minimum inherent error can be approximated using equation (2-3-38). A simple procedure for doing this is next outlined: The SOR computer program is executed for several versions of the microstrip configuration. Each version has the same strip width to height ratio above the ground plane; however, the number of lattice points is doubled for each succeeding execution. It is expected, after several iterations, that the inherent error is reduced to within an allowable limit. In other words, the benefit gained by doubling the grid size one additional time is assumed to have no substantial effects on the overall accuracy. In this research, the tolerances for the minimum residual and minimum inherent error were set to .001 and .01 volts, respectively. Using these tolerences in the SOR program, it was found that a mesh consisting of 60 horizontal and 40 vertical points produced results similar to those of Judd et-al. [7] for a microstrip having a width to height ratio

of one. The number of points representing the height and width were both twenty. It is interesting to note that the numerical results obtained by Judd et-al. [7] were calculated through an analytical approximation.

2.4 Calculation of the Characteristic Capacitance of a Microstrip

Once the potential field map in the region of the microstrip has been determined, the characteristic capacitance can be determined by employing Gauss' Law. The field map shown in Figure 11 depicts the discretized potential in the proximity of the microstrip. A discretization of Gauss' Law is used to approximate the charges on the microstrip. By applying similar steps to discretize the first derivative of the function f in section (2.3.2), and referring to the surface defined by the nodal points shown in Figure 12, an approximation to the electric displacement over the surface is:

$$E_n = \partial\varphi / \partial n = (\varphi_{i,j} - \varphi_o) / h \qquad (2\text{-}4\text{-}1)$$

where E_n is the normal component of the electric field intensity; n is the normal coordinate. The error in this approximation is again on the order of h^2; therefore, this is consistent with the finite difference process [6]. The flux density becomes

$$D_n = \varepsilon [(\varphi_{i,j} - \varphi) / h] \qquad (2\text{-}4\text{-}2)$$

where ε depends on the specific region. Next, Gauss' Law is applied, and the differential charge contained on the

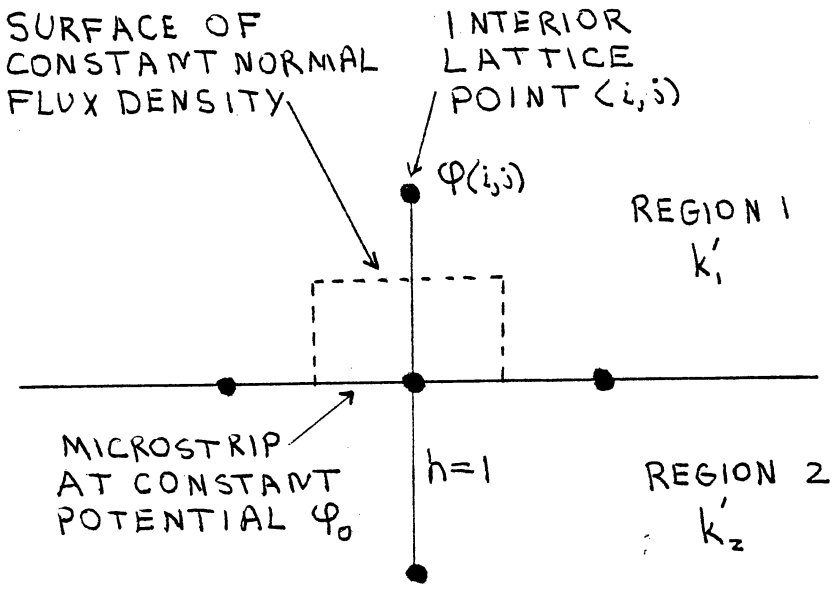

$$\Delta D_{n,i} = \epsilon_0 k'_1 (\varphi_0 - \varphi(i,j))$$

Figure 12. Integration Surface to Determine Charge Density

conducting differential portion of the surface can be calculated.

$$Q\ (i,j) = \varepsilon((\varphi_{i,j} - \varphi_o)\ /\ h)\ h \cdot L \qquad (2\text{-}4\text{-}3)$$

where L is the length of the microstrip perpendicular to the paper. The total charge on the two surfaces (top and bottom) becomes

$$Q_1 = \varepsilon_1\ L\ [\sum_{i,j}\ (\varphi_{i,j} - \varphi_o)] \qquad (2\text{-}4\text{-}4)$$

Similarly, Q_2 becomes

$$Q_2 = \varepsilon_2\ L\ [\sum_{i,j}\ (\varphi_{i,j} - \varphi_o)] \qquad (2\text{-}4\text{-}5)$$

The characteristic capacitances, C_1 and C_2, are next calculated from equations (2-4-4) and (2-4-5)

$$C_1 = Q_1/\varphi\varepsilon_o L = (k'_1/\varphi_o) \sum_{i,j}\ (\varphi_{i,j} - \varphi_o) \qquad (2\text{-}4\text{-}6)$$

and

$$C_2 = (k_2/\varphi_o) \sum_{i,j}\ (\varphi_{i,j} - \varphi_o) \qquad (2\text{-}4\text{-}7)$$

The total characteristic capacitance is the sum of C_1 and C_2.

$$C_T = C_1 + C_2 \qquad (2\text{-}4\text{-}8)$$

If the dielectric medium is inhomogeneous, two steps are necessary to calculate the characteristic capacitance [6]. First the capacitance is calculated for the case with all dielectrics removed, i.e., $k'_1 = k'_2 = 1$. The next step is to insert the dielectrics and recalculate the capcitance. Finally, the characteristic capacitance is found by taking the geometric mean of these two values. According to Green [6], the characteristic capacitance becomes:

$$C^* = (C_o C)^{\frac{1}{2}} \qquad (2\text{-}4\text{-}9)$$

where C_o is the capacitance without dielectrics, and C is the capacitance with dielectrics present. To calculate the capacitance for a given length of microstrip, the equation becomes

$$C^* = (C_o C)^{\frac{1}{2}} (L)(\varepsilon_o) \quad \text{Farads} \qquad (2\text{-}4\text{-}10)$$

where L is the length of the microstrip, and ε_o is the permitivity of free space. Equations (2-4-9) and (2-4-10), have been incorporated into a SOR computer program and a FORTRAN listing of this program is given in the Appendix. To test the SOR computer program, several microstrip geometries, having different width to height ratios, were constructed and tested. A vector impedance meter was used to measure the microstrip's impedance. The reactance component was next calculated through a set of equations given by the impedance meter's manufacturer; this procedure compensates for the parasitic effects of the meter's probe. The dielectric materials for the upper and lower regions were styrofoam and plexiglas, respectively. Due to buckling of the copper-clad printed circuit board, the styrofoam provided a good contact between the copper and plexiglas surface. Figure 13 shows a simplified schematic of the test arrangement. The total length, L, of the microstrip is 66 inches. The dielectric constants for plexiglas and styrofoam at 1 MHz are 2.76 and 1.03, respectively [3]. A plot of both the measured and calculated capacitances versus microstrip width to height ratios is shown in Figure 14. The results shown in this

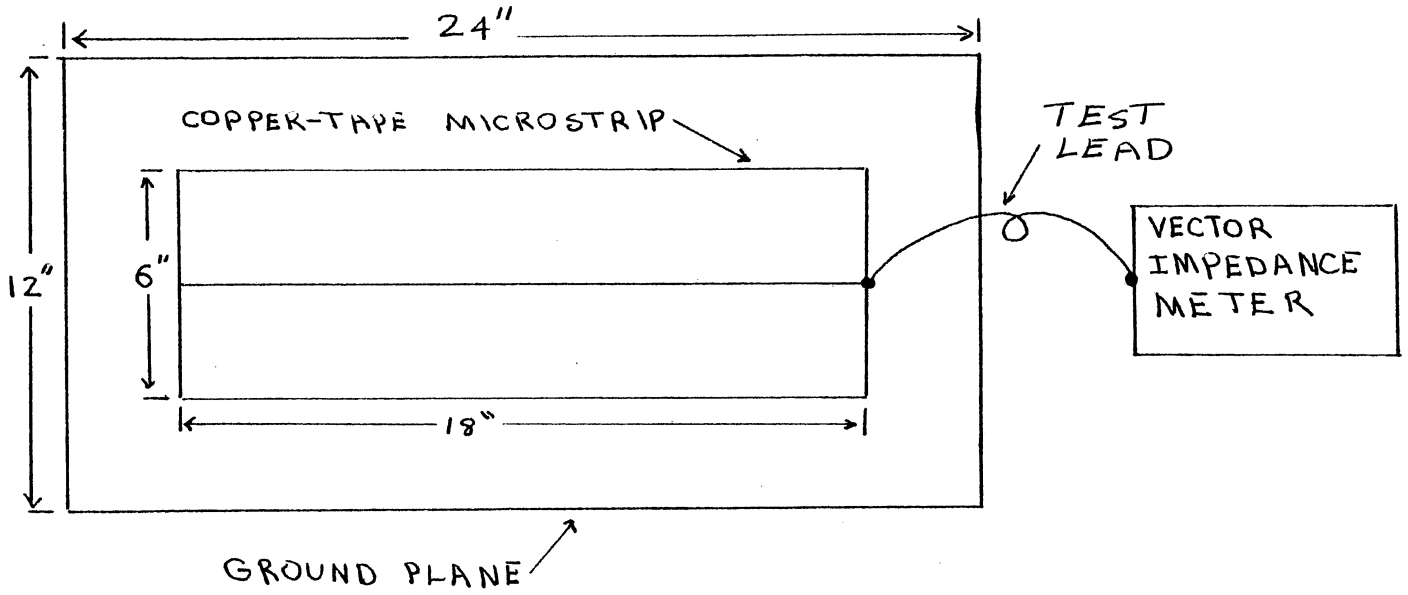

Figure 13. Microstrip Capacitance Test Arrangement.

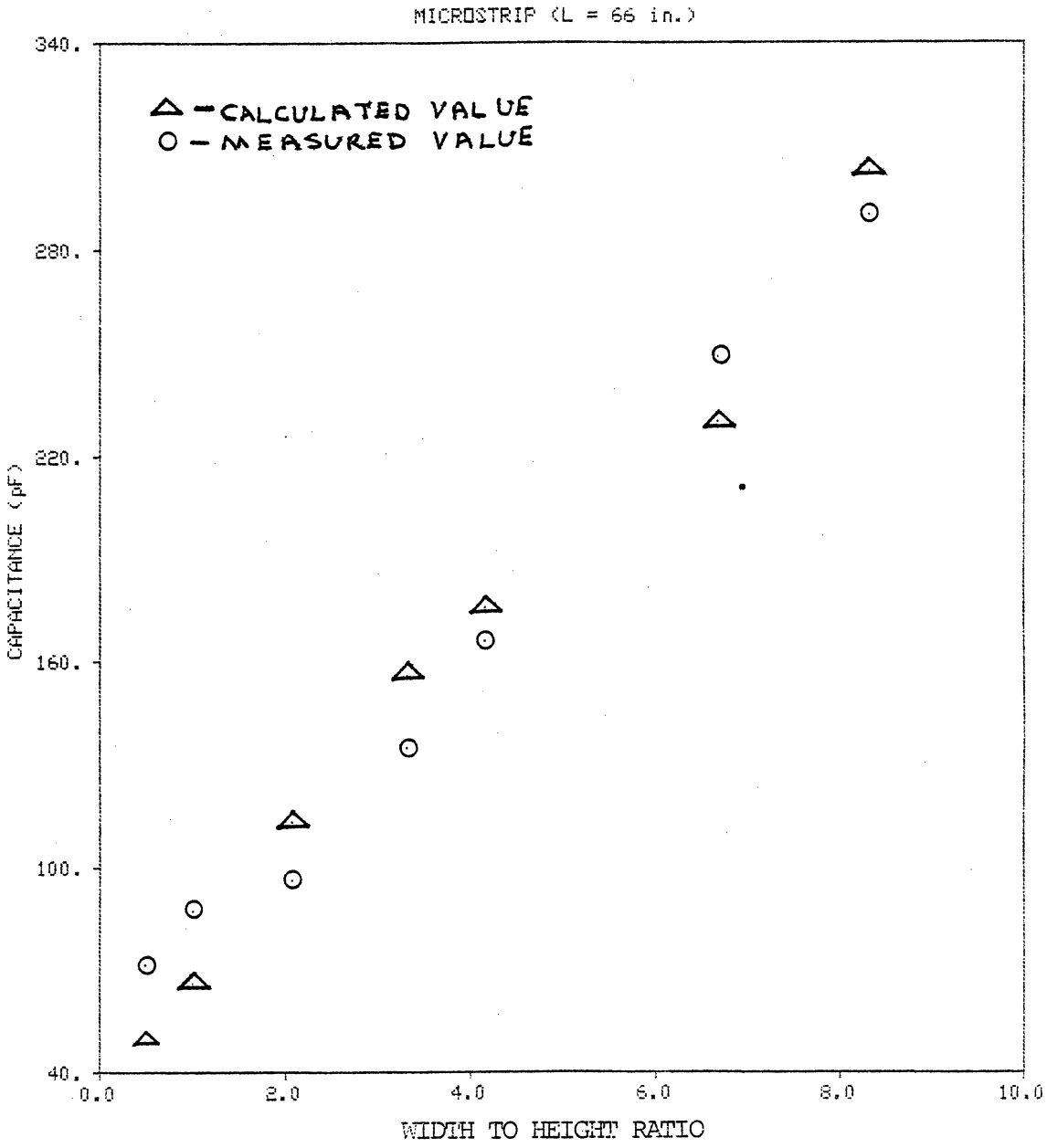

Figure 14. Plot of Calculated and Measured Capacitance Values Versus Width to Height Ratio.

figure indicate that the technique used to calculate these values is capable of providing reasonable approximations of the microstrip's capacitance.

Using the analytical technique discussed, it is now possible to calculate theoretical approximations to the sensitivity factors using values for k'_1 and k'_2 given in published data. Table 1 shows the values for k'_1 extracted from Figure 4(a). Due to the natural variation in wheat, these values are considered to be only approximate with regard to the wheat samples used in this research. However, these values adequately represent a typical range of the dielectric constant of wheat at a frequency of 1 MHz and over a moisture range of 8.3 to 17.9%. Figure 15 shows a plot of the calculated SF's, given in percent, against moisture content. The next section discusses the significance of this figure and the differences in SF for the two test cells.

2.5 Results and Discussion

The objective of the last few sections of this chapter has been to develop a quantitative criterion on which to judge the theoretical 'performance' of a microstrip as a moisture sensor for grain. Consequently, a technique was required to calculate an approximation of the microstrip's characteristic capacitance. This was accomplished through the SOR computer program.

Restated, the SF is defined as the fraction of k' that

TABLE I

DIELECTRIC CONSTANT OF HARD RED WINTER WHEAT AT 1 MHz [2]

Moisture Content (%, wet-basis)	k'
8.3	3.73
10.5	4.10
12.7	4.67
14.4	4.87
16.2	5.17
17.9	5.83

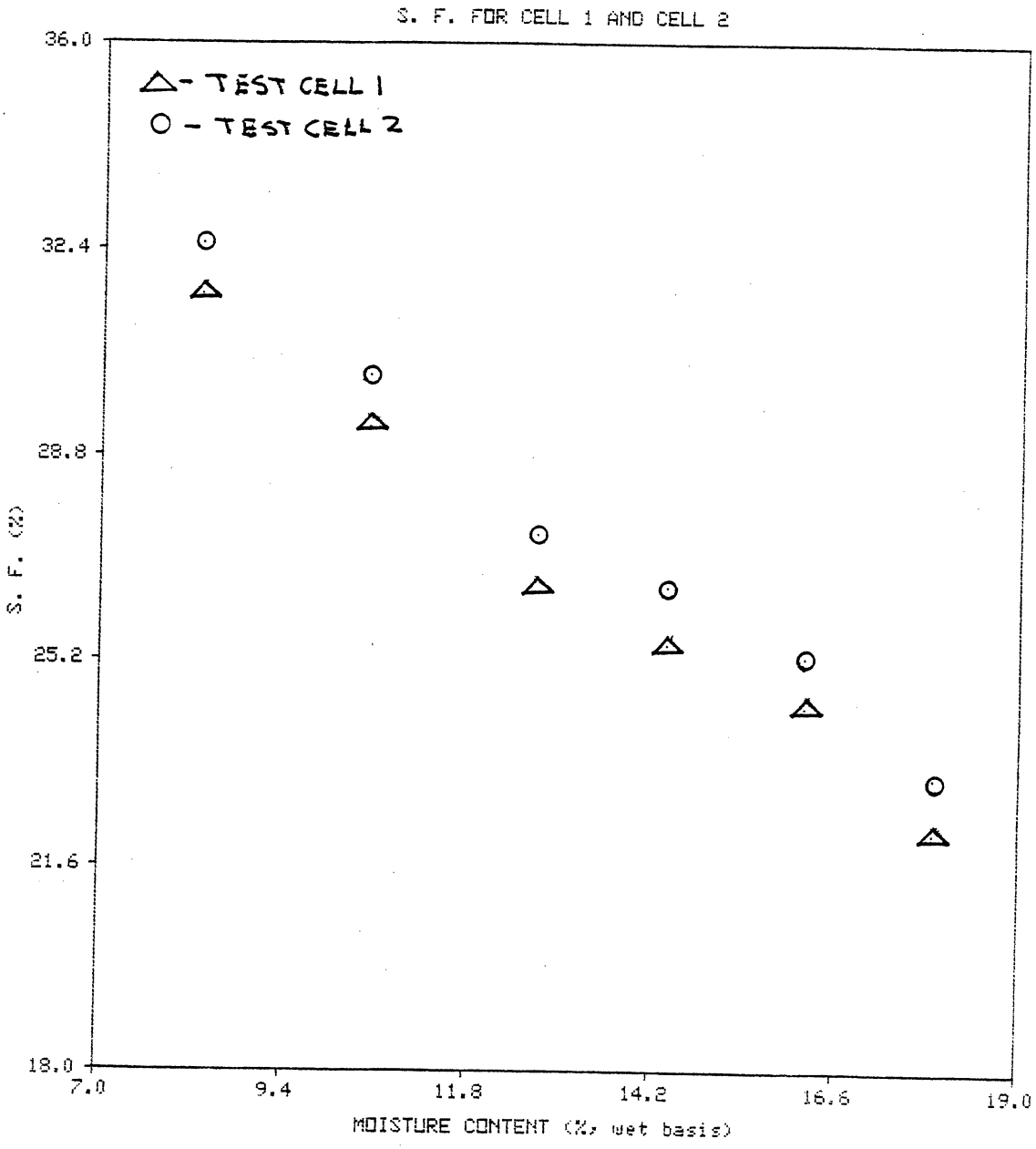

Figure 15. Plot of Sensitivity Factors for Test Cell 1 and Test Cell 2

affects the microstrip's capacitance as the dielectric medium in region 1 is changed from air to wheat. The reduction of the SF could be viewed as a degradation of k'_1 as an influence on the capacitance. Since the underlying premise is to sense a change in moisture content, this measurement is likewise degraded. Referring to Figure 15, it becomes apparent neither cell has a very impressive SF. In fact, it can be observed in this Figure that the SF decreases from roughly 33% to 22% going from the driest to wettest moisture content. A crucial point in this problem occurs when fluctuations in capacitance, due to changes in moisture content, approach the standard measurement error of the moisture meter. Therefore, this inherent deficiency in microstrip sensors limits their application according to the desired degree of resolution in the measurement of moisture content. This insensitivity of microstrips was expected due to the nature of the fringe-field. However, Figure 15 does indicate a preference for cell 2 over cell 1 since its SF is consistently higher. Unfortunately, the SF differs only by a small amount.

The next chapter deals with the construction and testing of the two proposed cells. The goals of Chapter III are to determine whether a fringe-field device, like a microstrip, is capable of sensing changes in the moisture content of wheat and if a significant difference exists between the performance of the two cells.

CHAPTER III

CONSTRUCTION AND TESTING OF THE MICROSTRIP CAPACITANCE CELL AS A MOISTURE SENSOR

3.1 Introduction

This chapter deals with the construction and testing of the two proposed capacitance test cells. In chapter II, a sensitivity factor, SF, was derived on a theoretical basis, and values for the SF were calculated for each cell using published data for the dielectric constants of wheat and of plexiglas. From this analysis, it was asserted that test cell 2 should have better sensitivity to changes in the wheat's moisture content as opposed to test cell 1. The objective of this chapter is to test this hypothesis in the laboratory. The tests are performed by electrically coupling the test cell to an impedence meter and measuring the cell's impedance for several samples of wheat that have various preconditioned moisture contents. Next, the cell's sensitivity is evaluated according to how well its capacitance measurements are correlated to the moisture content.

3.2 Design and Construction

The lab experiment began by procuring a supply of

recently harvested and cleaned hard red winter wheat, a common type grown in Oklahoma. For testing purposes, six samples of wheat ranging in moisture content were prepared. This range was considered to be typical, and problems inherent with grain storage become increasingly critical as the moisture content in wheat rises above ten percent.

The moisture content of the wheat supplied for this research was measured at 10.3%, thus establishing the lower limit of moisture content and also providing the first wheat sample. The remaining five samples were prepared by adding the required amount of water to raise its moisture content to the desired level. The definition for moisture content used in this research is established on a wet basis.

MC = mass of water in sample/total mass of sample (3-2-1)

The following steps were taken to produce the various moisture contents.

(1) The moisture content, MC, and mass, M, of the sample are measured.

(2) The mass of water needed to raise the MC is next calculated.

$$MC_1 = W_1 / M_1 \quad (3\text{-}2\text{-}2)$$

$$MC_2 = W_2 / M_2 = (W_1 + \Delta W) / (M_1 + \Delta W) \quad (3\text{-}2\text{-}3)$$

where W represents the mass of water, and the subscripts, 1 and 2, signify the original and desired conditions of the sample, respectively. Through algebraic manipulations of

equations (3-2-2) and (3-2-3), and solving for ΔW, the weight of required water becomes

$$\Delta W = M_1(MC_2-MC_1)/(1-MC_2) \qquad (3\text{-}2\text{-}4)$$

After adding the required amount of water, the samples were sealed in one-quart glass jars and kept in a refrigerator for approximately one week allowing the water to become evenly distributed. Table 2 gives the measured moisture contents of the samples.

The test cells were constructed from readily available materials. Plexiglas was chosen as the substrate dielectric because it has stable physical and electrical properties. In addition, plexiglas is easy to machine and not overly expensive compared to similar construction materials. The complete test cell apparatus consists of a few basic items: the ground plane is approximated by a sheet of copper-clad printed circuit board; resting on top of the ground plane is an open top plexiglas box to confine the wheat sample; adhesive copper tape, applied on the inner-bottom surface of the box, functions as the microstrip. This arrangement permits the wheat to come into contact with the electrodes. Figure 16 shows a perspective view of this device, and Table 3 gives the dimensional details. The second test cell is simply a modification of the first. Since the only physical difference in the two cells is the thickness of the plexiglas substrate, an additional sheet of plexiglas is placed between the ground plane and the plexiglas of the

TABLE II

PRECONDITIONED MOISTURE CONTENTS

Sample	Moisture Content (%, wet-basis)
1	10.3
2	11.1
3	12.0
4	12.5
5	13.0
6	14.0

TABLE III

TEST CELL PHYSICAL DIMENSIONS

Description	Dimension
Ground Plane	12" x 24" x 1/16"
Plexiglas Sheet (substrate)	12" x 24" x 1/16" (cell 1)
	12" x 24" x 1/8" (cell 2)
Plexiglas Box (1/8" plexiglas)	6" x 6" x 3"
Strip Line (copper tape)	1/8" x 34" x 30/1000"

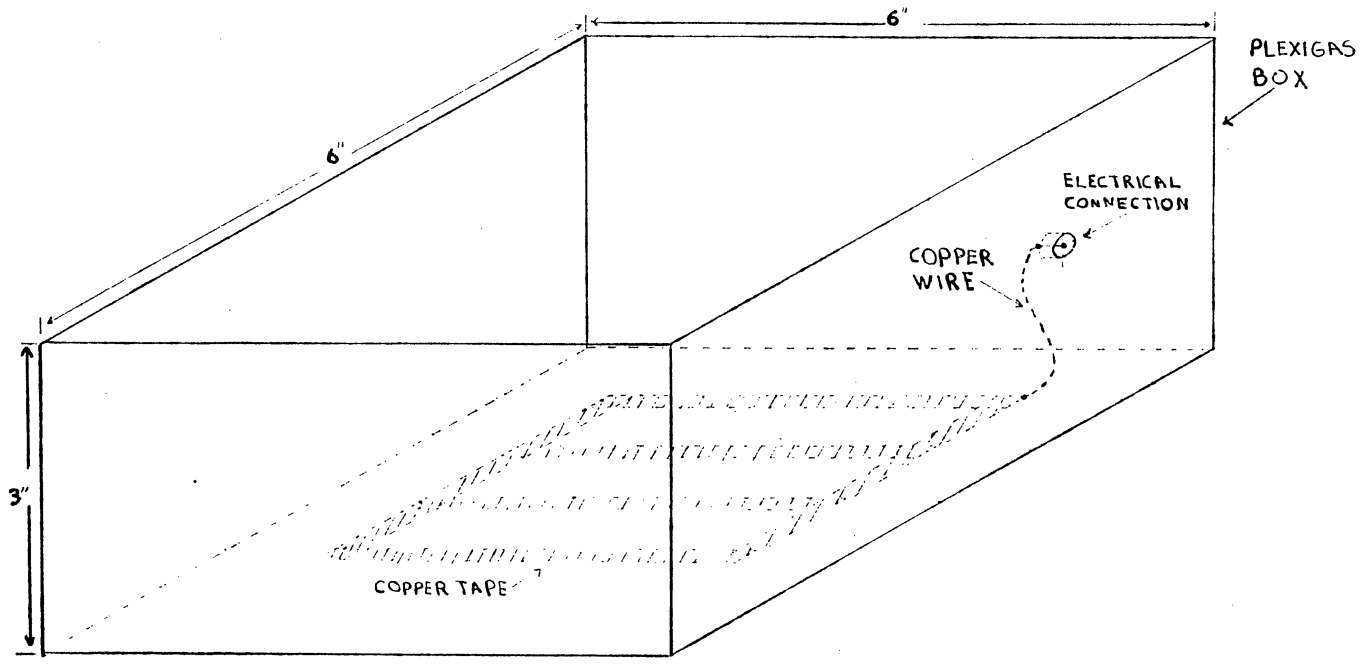

Figure 16. Perspective View of Test Cell Apparatus.

bottom of the box.

3.3 Lab Measurements

In order to minimize the time dependency in the lab measuring process, the wheat samples were assigned numbers ranging from 1 through 6. A random number generator was used to establish the order in which the samples were to be tested. A total of 60 measurements were taken, and each sample was measured ten times in a random fashion. It should be noted that special care was taken when filling the test cells. This was done to insure consistency in the settling of the wheat grains, thus attempting to minimize the measurement error. Additionally, the wheat grains accumulate a large static charge when poured from a glass container. This was noticable since an electric shock could be felt when touching the electrode, immediately after filling the cell. To reduce the static charge build up, the wheat was first poured into a grounded metal container and then into the test cell. This considerably reduced the static charge. Figure 17 shows a plot of the capacitance versus moisture content (i.e. percent, wet basis) for test cell 1. Similarly, Figure 18 shows a plot of the data for test cell 2.

In order to explore the inherent relationship between the measured capacitance values and the measured moisture contents as shown in Figures 17 and 18, a simple linear regression is performed on these two data sets. The

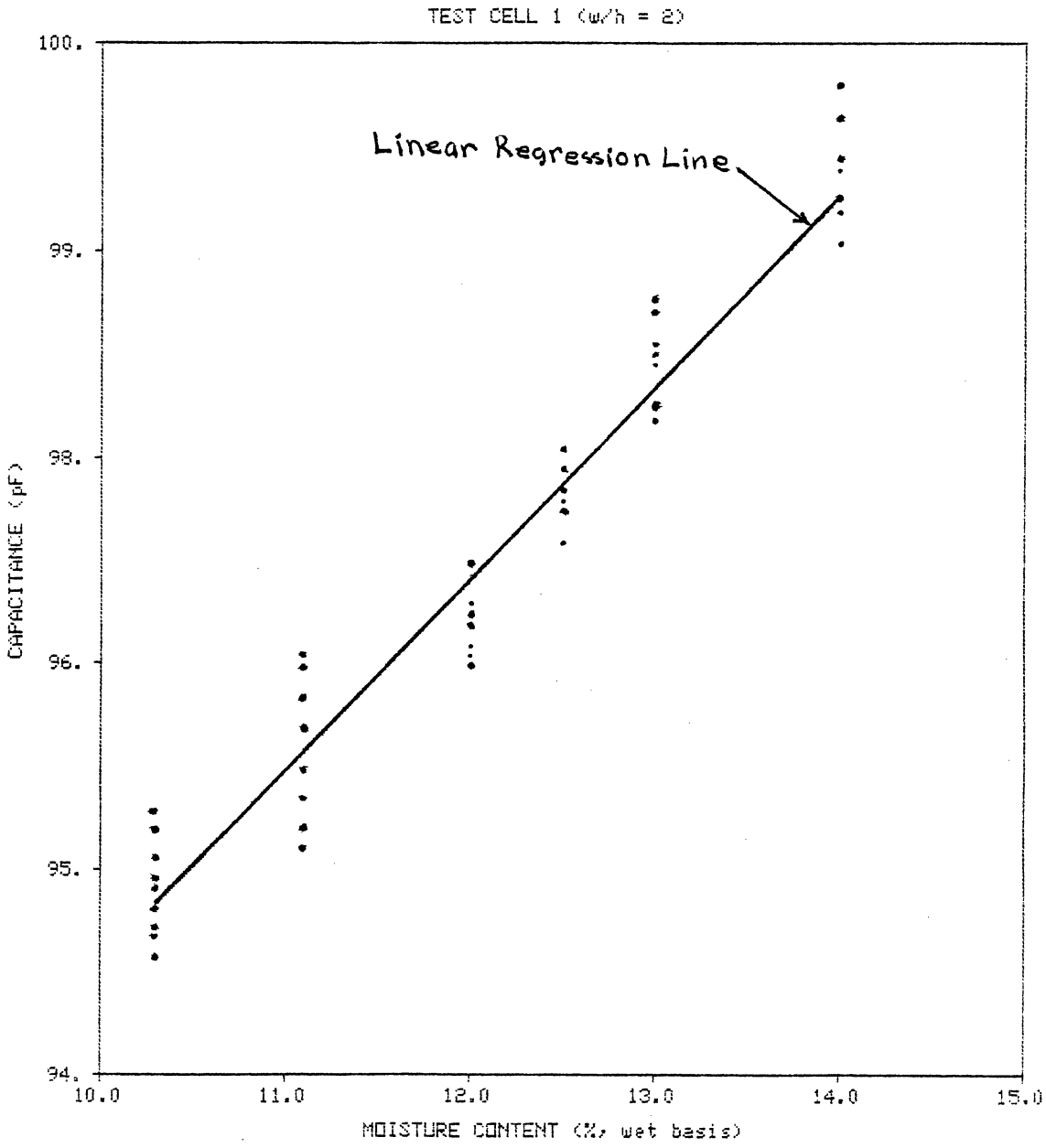

Figure 17. Plot of Measured Capacitance Versus Moisture Content for Test Cell 1.

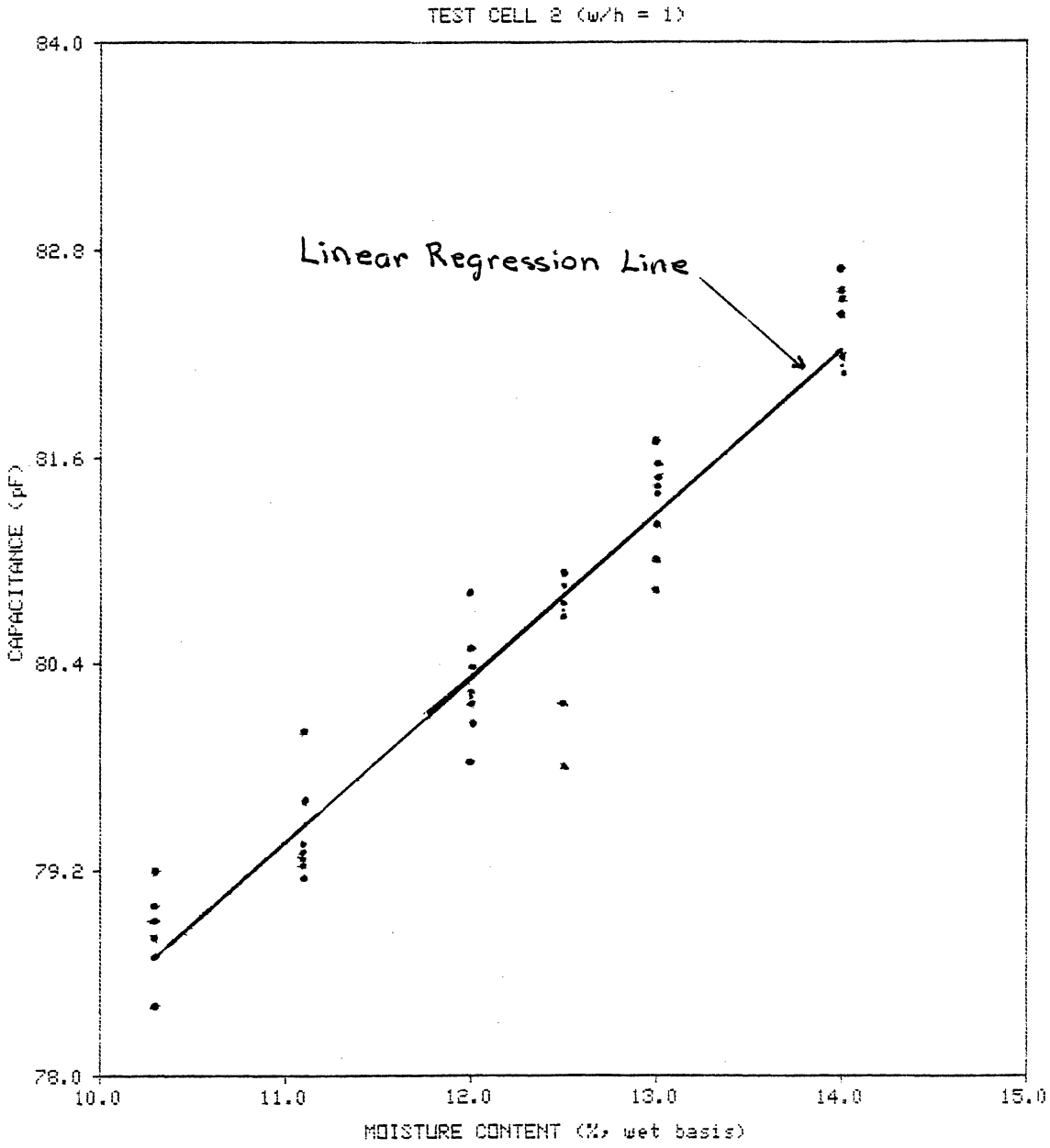

Figure 18. Plot of Measured Capacitance Versus Moisture Content for Test Cell 2.

coefficient of determination, R^2, can be defined as the square of the correlation coefficient between the capacitance values and the moisture content values. In other words, R^2 is a measure, as a fraction, of the variation in the data accounted for by the regression.

$$R^2 = SS_R / S_{yy} \quad (3\text{-}3\text{-}1)$$

where SS_R is the regression sum of squares, and S_{yy} is the sum of squares for y, i.e., the capacitance values. The respective R^2 values for test cells 1 and 2 are

$$R^2_1 = 0.953 \quad (3\text{-}3\text{-}2)$$

$$R^2_2 = 0.941 \quad (3\text{-}3\text{-}3)$$

The estimated slopes, m, for the two regression lines are:

$$m_1 = 1.12 \ \text{pF/MC} \quad (3\text{-}3\text{-}4)$$

$$m_2 = 0.953 \ \text{pF/MC} \quad (3\text{-}3\text{-}5)$$

and their respective variances are:

$$V_1 = 1.06 \times 10^{-3} \ (\text{pF})^2 \quad (3\text{-}3\text{-}6)$$

$$V_2 = .980 \times 10^{-3} \ (\text{pF})^2 \quad (3\text{-}3\text{-}7)$$

These results indicate that it is possible to sense changes in the wheat's moisture content. However, they also reveal that test cell 1 appears to have better sensitivity characteristics than cell 2. This is in disagreement with the predictions made in Chapter 2. An attempt is made in the next section to explain this discrepancy.

3.4 Comparison of Theoretical and Experimental Results

The statistics presented in the last section point out

the possibility that cell 1 could be the preferred choice over cell 2 as a moisture sensor. A discrepancy exists between the theoretical and measured performances. Two explanations are offered: (i) it is quite likely that the experimental procedures for cell 2 were less consistent, thus contributing to a greater variance in the measurements (this is evident when comparing the dispersion in the data plots, see Figures 17 and 18): and (ii) perhaps less critical, is the lower capacitance values of cell 2 which could increase the effects of stray lead capacitances. Since the slopes of the regression lines were derived from measured data containing measurement error, two situations requiring statistical inference are needed: to determine whether or not (i) the two slopes are significantly different from each other and (ii) the slopes are significantly greater than zero [12]. Before proceeding with the hypothesis testing, it is assumed that a sufficient number of measurements have been taken, and the mesurement errors are independent and Normally distributed with zero mean and constant variance. To simplify the hypothesis testing, it can be shown that the sample variances of the two slopes are statistically equivalent.

The first hypothesis test provides a statement about the similarity between the slopes. This is important, because if the slopes were equivalent one would have to conclude that both test cells have the same sensitivity. This hypothesis test follows the t-distribution with a

significance level of α and $n_1 + n_2 - 2$ degrees of freedom. The integers n_1 and n_2 are the number of random samples taken for the respective test cells. Both n_1 and n_2 are equal to sixty in this study, and for practical purposes

$$n_1 + n_2 - 2 \approx 120 \qquad (3\text{-}3\text{-}8)$$

The null hypothesis, H_o, is defined as the hypothesis that m_1 equals m_2, and the alternative hypothesis is the hypothesis that m_1 is greater than m_2.

$$H_o = m_1 = m_2 \qquad (3\text{-}3\text{-}9)$$

$$H_1 = m_1 > m_2 \qquad (3\text{-}3\text{-}10)$$

The t-test becomes

$$t_o = (m_1 - m_2)/[S_p(1/n_1 + 1/n_2)^{\frac{1}{2}}] \qquad (3\text{-}3\text{-}11)$$

where S_p^2 is the combined (or 'pooled') estimator of the population variance.

$$S_p^2 = [(n_1-1)V_1 + (n_2-1)V_2]/(n_1+n_2-2) \qquad (3\text{-}3\text{-}12)$$

where V_1 and V_2 are the sample variances of the slopes m_1 and m_2, respectively. Inserting the appropriate values into equation (3-3-11), the t-test becomes

$$t_o = 28.6 \qquad (3\text{-}3\text{-}13)$$

$$t_{.05,120} = 1.66 \qquad (3\text{-}3\text{-}14)$$

Since t_o is greater than $t_{.05,120}$, it can be stated that there is sufficient evidence to reject the null hypothesis that m_1 equals m_2. Therefore, m_1 is greater than m_2 with 95 percent confidence.

The next hypothesis test concerns the significance of the regression. The question asked is whether or not the two slopes are significantly different from zero. This

test follows the $F_{\alpha,1,n-2}$ distribution [12]. The hypothesis test is

$$H_o: \quad m = 0 \tag{3-3-15}$$

$$H_1: \quad m = 0 \tag{3-3-16}$$

The F-test is

$$F_o = MS_R \; / \; MS_E \tag{3-3-17}$$

where MS_R is the sum of squares of the regression, and MS_E is the sum of squares of the error (or residual). The above null hypothesis is rejected if

$$F_o > F_{.025,1,60} = 7.08 \tag{3-3-18}$$

For test cell 1 F_o is

$$F_o = 1180. \tag{3-3-19}$$

and for test cell 2 F_o is

$$F_o = 916. \tag{3-3-20}$$

From equations (3-3-18), (3-3-19), and (3-3-20) it is evident that the null hypothesis must be rejected, and it can be stated that both slopes are significantly different from zero with 95 percent confidence.

CHAPTER IV

SUMMARY AND CONCLUSIONS

4.1 Summary of Results and Conclusions

The moisture content in cereal grains such as wheat is an essential factor in the quality, storage, and processing of this important agricultural commodity. Methods continue to be invented or improved to provide reliable and accurate measurements of moisture content. This thesis studies a microstrip geometry as a moisture sensor. Although it may be applicable to many products where moisture content is a critical issue, wheat was selected for this study since it is one of the predominant cereal grains grown in Oklahoma.

Numerous challenges arise when dealing with agricultural products, and as one might expect, this is primarily due to nature's unpredictable behavior. Two difficulties encountered in this study were in the modeling of wheat as a dielectric material and the variations in the wheat's bulk density.

The primary objective of this thesis was to evaluate a fringe-field device as a moisture sensor for grain. Due to its simple geometry, the microstrip configuration was

selected as the fringe-field moisture sensor. A sensitivity factor was defined in terms of the characteristic capacitance and the dielectric constant of the region above the strip. This assisted in establishing a design criteria for microstrip capacitance cells. Essential to the calculation of the characteristic capacitance is a successive overrelaxation technique used to solve finite difference equations with one boundary at infinity. A discussion of this technique was presented. Lab tests confirmed the approximations employed by this technique for selected microstrip configurations. Consequently, this technique could be applied to more general configurations of microstrip design. A FORTRAN listing is given in the Appendix. The results documented in Chapter III provide evidence that a fringe-field device can capably function as a moisture sensor, provided that a relatively sensitive instrument is used to measure the changes in the cell's capacitance. However, the microstrip is limited by its lack of sensitivity to changes in the dielectric properties of the material in the region above the strip. This was expected due to the dispersed nature of the fringe-field. For practical uses, it can be stated that the microstrip configuration is adequate as a moisture sensor for wheat, but how well it performs is subject to the degree of the desired resolution in the moisture measurement. Further work is needed to develop a fringe-field geometry and/or substrate combination that would yield a 'robust' moisture

sensor.

4.2 Scope for Further Work

Further work in the area of fringe-field moisture sensors could pertain to developing a device that is sensitive to changes in its fringe-field and yet maintains the desired nonintrusive quality of these devices. Perhaps the techniques presented in this thesis will aid in the investigation of other geometries, besides the microstrip, as moisture sensors. An infinite number of possible geometric schemes exist.

SELECTED BIBLIOGRAPHY

[1] Nelson, S. O. "Electrical Properties of Agricultural Products - A Critical Review." Transactions of the American Society of Agricultural Engineers, Vol. 16(2) (1973), pp. 384-400.

[2] Nelson, S. O. "Factors Affecting the Dielectric Properties of Grain." Transactions of the American Society of Agricultural Engineers, Vol. 25(2) (1982), pp. 1045-1049,1056.

[3] Von Hipple, A. R. "Theory, Macroscopic Properties of Dielectric Materials and Applications." Dielectric Materials and Applications. Ed. Arthur Von Hipple, John Wiley and Sons, Inc. 1959, pp. 3-9.

[4] Matthews, J. "The Design of an Electrical Capacitance-Type Moisture Meter For Agricultural Use." National Institute of Agricultural Engineers, (1962), pp. 17-30.

[5] Wexler, Alvin "Computation of Electromagnetic Fields." IEEE Transactions on Microwave Theory and Techniques, Vol. MTT-17, No.8, (August 1969), pp. 416-439.

[6] Green, Harry E. "The Numerical Solution of Some Important Transmission-Line Problems." IEEE Transactions on Microwave Theory and Techniques, Vol. MTT-13, No. 5, (September 1965), pp. 676-692.

[7] Judd, S. V., Whiteley, I., Clowes, R. J., and Rickard, D. C. "An Analytical Method For Calculating Microstrip Transmission Line Parameters." IEEE Transactions on Microwave Theory and Techniques, Vol. MTT-18, No. 2, (February 1970) pp. 76-87.

[8] Sandy, F. and Sage, J. "Use of Finite Difference Approximations For Problems Having Boundaries At Infinity." IEEE Transactions on Microwave Theory and Techniques, Vol. MTT-19, No. 5, (May 1971), pp. 484-486.

[9] Silvester, P. Modern Electromagnetic Fields, Prentice-Hall, Inc. 1968, pp. 56-65.

[10] Gerald, C. F. and Wheatley, P. O. Applied Numerical Analysis, Reading Massachusetts, Addison-Wesley Publishing Company, 1985, Chapter 7.

[11] Scarborough, J. B. Numerical Mathematical Analysis, Baltimore, The Johns Hopkins Press, 6th ed, 1966, Chapter XIV.

[12] Hines, W. W. and Montgomery, D. C. Probability and Statistics in Engineering and Management Science, John Wiley and Sons, 1980, Chapter 12.

APPENDIX

FORTRAN LISTING OF SOR COMPUTER PROGRAM

```
C     ****************************************************************
C          CAP.FOR
C
C          ITERATION PROGRAM FOR THE APPROXIMATIONS TO PARTIAL
C     DIFFERENTIAL EQUATIONS FOR A MICRO STRIP HAVING A
C     BOUNDARY AT INFINITY.
C
C     ****************************************************************
      REAL V(40,60),Q(59),VB(98),ALPHA,RESMAX,R,X,Y,Y1,Y2,Z
     $     ED1,ED2
      INTEGER FLAG,H,W,WN
      DATA PI,RESMAX,ALPHA/6.283,1.E-3,1.834/
      OPEN (UNIT=20,NAME='VOLTS.DAT',STATUS='NEW')
      OPEN (UNIT=21,NAME='CAP.DAT',STATUS='NEW')
C


 77     PRINT *,' Enter the height of the top conductor.'
        PRINT *,' H='
        READ *,H
C
        PRINT *,' Enter the half width of the conductor.'
        PRINT *,' W='
        READ *,W
C
        PRINT *,' Enter the permittivities of regions 1 and 2.'
        PRINT *,' ED1 (top region) = '
        READ *,ED1
        PRINT *,' ED2 = '
        READ *,ED2
C
        WRITE(6,99) H,W,ED1,ED2
  99    FORMAT(1X,'The height is ',I2,' half width is ',I2,
     $ ' ED1 (top region) = ',F5.2,' ED2 = ',F5.2)
C


C
C     DATA FILE CONTAINS W,H, AND E1,E2 .
C

      DO 20 I=1,40
        V(I,60) = 4.
        DO 21 J=30,59
  21      V(I,J) = 6.
  20    CONTINUE
C
      DO 22 J=30,60
        V(1,J) = 4.
        V(40,J) = 0.
  22    CONTINUE
C
```

```
      L = W + 30
      K = 40 - H
      DO 23 J=30,L
   23   V(K,J) = 9.
C
C     ITERATION CYCLE
C
      KOUNT = 1
      R = ALPHA/4.
C
    1 INDIC = 0
      FLAG = 0
      DO 2 I=2,K-1
        RES = 2.*V(I,31) + V(I-1,30) + V(I+1,30) - 4.*V(I,30)
        IF(ABS(RES) .GE. RESMAX) INDIC = 1
        V(I,30) = V(I,30) + R*RES
        DO 3 J=31,59
          RES = V(I,J-1) + V(I-1,J) + V(I,J+1) + V(I+1,J) - 4.*V(I,J)
          IF(ABS(RES) .GE. RESMAX) INDIC = 1
          V(I,J) = V(I,J) + R*RES
    3     CONTINUE
    2   CONTINUE
C
      DO 4 J=L+1,59
        RES = (2.*ED2/(ED2+ED1))*V(K+1,J) + (2.*ED1/(ED1+ED2))*V(K-1,J)
     $        + V(K,J-1) + V(K,J+1) - 4.*V(K,J)
        IF(ABS(RES) .GE. RESMAX) INDIC = 1
        V(K,J) = V(K,J) + R*RES
    4   CONTINUE
C
      DO 5,I=K+1,39
        RES = 2.*V(I,31) + V(I-1,30) + V(I+1,30) - 4.*V(I,30)
        IF(ABS(RES) .GE. RESMAX) INDIC = 1
        V(I,30) = V(I,30) + R*RES
        DO 6 J=31,59
          RES = V(I,J-1) + V(I-1,J) + V(I,J+1) + V(I+1,J) - 4.*V(I,J)
          V(I,J) = V(I,J) + R*RES
    6     CONTINUE
    5   CONTINUE
C
      KOUNT = KOUNT + 1
      IF (KOUNT .GE. 600) GO TO 15
      IF (INDIC .EQ. 1) GO TO 1
C
      Q(30) = (V(K-1,30) + V(K+1,30) - 18.) / PI
      DO 8 J=31,59
        Q(J)= (V(K-1,J) + V(K+1,J) + V(K,J-1) + V(K,J+1) - 4.*V(K,J))/PI
        Q(60-J) = Q(J)
    8   CONTINUE
C
      Y1 = (K-1.)**2.
```

```
      Y2 = (H+39.)**2.
      DO 10 N=30,60
        VB(N) = 0.
        DO 11 J=1,59
          X = (N-J)**2.
          Z = SQRT((X+Y1)/(X+Y2))
          VB(N) = VB(N) + Q(J)*ALOG(Z)
 11       CONTINUE
        RES = VB(N) - V(1,N)
        IF(ABS(RES) .GE. RESMAX) FLAG = 1
        V(1,N) = VB(N)
 10     CONTINUE
C
      DO 12 N=61,98
        Y = N-59.
        VB(N) = 0.
        DO 13 J=1,59
          X = (J-60.)**2.
          Y1 = (Y-H)**2.
          Y2 = (Y-(H+40))**2.
          Z = SQRT((X+Y1)/(X+Y2))
          VB(N) = VB(N) + Q(J)*ALOG(Z)
 13       CONTINUE
        M = N-59
        RES = VB(N) - V(M,60)
        IF(ABS(RES) .GE. RESMAX) FLAG = 1
        V(M,60) = VB(N)
 12     CONTINUE
C
      IF(FLAG .EQ.1) GO TO 1
C
C     *** SUM1 = TOTAL VOLTAGE ABOVE CONDUCTOR ***
 15   SUM1 = 0.
C     *** SUM2 = TOTAL VOLTAGE BELOW CONDUCTOR ***
      SUM2 = 0.
      DO 14 J=31,L
        SUM1 = SUM1 + V(K-1,J)
        SUM2 = SUM2 + V(K+1,J)
 14     CONTINUE
C
      SUM1 = ( 18.*(W+1) - ( V(K-1,30) + V(K,L+1) + 2.*SUM1 ) )
      CAP1 = ED1*SUM1 / 9.
      SUM2 = ( 18.*(W+1) - ( V(K+1,30) + V(K,L+1) + 2.*SUM2 ) )
      CAP2 = ED2*SUM2 / 9.
      CAPT = CAP1 + CAP2
C
      WN = 2*W
C
      PRINT *,' THE NUMBER OF ITERATIONS IS = ',KOUNT
      WRITE(6,100) CAP1,ED1,CAP2,ED2,CAPT,H,WN,KOUNT
C
```

```
      WRITE(21,100) CAP1,ED1,CAP2,ED2,CAPT,H,WN,KOUNT
C
      WRITE(20,100) CAP1,ED1,CAP2,ED2,CAPT,H,WN,KOUNT
C
  100 FORMAT(/,5X,'CAP1 = ',F7.3,' ED1 = ',F5.2,/,
     &          5X,'CAP2 = ',F7.3,' ED2 = ',F5.2,/,
     &          5X,'CAPT = ',F7.3,' H = ',I2,3X,' W = ',I2,/,
     &          5X,'NO. OF ITERATIONS = ',I3,/)
C
      PRINT *,' TO CONTINUE, ENTER 1; ELSE, ENTER 0'
      PRINT *,' ???? '
      READ *, II
      IF(II .EQ. 1) GO TO 77
   67 CLOSE (UNIT=20,STATUS='KEEP')
      CLOSE (UNIT=21,STATUS='KEEP')
C
      STOP
      END
```

VITA

Paul Walton Hein

Candidate for the Degree of

Master of Science

Thesis: AN ANALYSIS OF A MICROSTRIP DEVICE AS A MOISTURE SENSOR FOR GRAIN

Major Field: Electrical Engineering

Biographical:

Personal Data: Born in Lawton, Oklahoma, December 29, 1960, the son of Vernon L. and Emmi Hein. Married to Rebecca A. Sutko on May 25, 1985.

Education: Graduated from Eisenhower High School, Lawton, Oklahoma, in May, 1979; received Associate of Technology Degree from Cameron University, Lawton in May, 1981; received Bachelor of Science Degree in Electrical Engineering from Oklahoma State University in May, 1985; completed requirements for the Master of Science degree at Oklahoma State University in July, 1987.

Professional Experience: Electrical Engineer, Frontier Engineering, Inc., Stillwater, Oklahoma, May, 1985 to January,1986; Paraprofessional, Department of Agricultural Engineering, Oklahoma State University, May, 1986 to August, 1986; Graduate Assistant, Department of Electrical Engineering, Oklahoma State University, August, 1985 to May, 1987.

Professional Organizations: Member of the Institute of Electrical and Electronics Engineer, Eta Kappa Nu.